Electronic Supplementary Information

Tetralactam macrocycle based indicator displacement assay for colorimetric and fluorometric dual-mode detection of urinary uric acid

Huan Yao,†[a] Shi-Yao Li,†[a] Hong Zhang,[b] Xin-Yu Pang,[b] Jia-Le Lu,[a] Cong Chen, [c] Wei Jiang,‡[b] Liu-Pan Yang,*[a] and Li-Li Wang*[a]

[a.] School of Pharmaceutical Science, Postdoctoral Research Station of Basic Medicine, Hengyang Medical School, University of South China, Hengyang, Hunan, 421001, China. E-mail: yanglp@usc.edu.cn, wangll@usc.edu.cn.

[b.] Department of Chemistry, Southern University of Science and Technology, Xueyuan Blvd 1088, Shenzhen, 518055, China.

[c.] Department of Clinical Laboratory Medicine, Institution of Microbiology and Infectious Diseases, The First Affiliated Hospital, Hengyang Medical School, University of South China, Hengyang, Hunan, 421001, China.

† These authors contributed equally to this work.

‡ deceased (2022.12)

CONTENT

1. Experimental Section

1.1 General Method

All the guest molecules involved in this research were commercially available and used without further purification unless otherwise noted. Solvents were either employed as purchased or dried prior to use by standard laboratory procedures. Ultrapure water was purified from Chuangchun pure water machine CCH-H200. ^{1}H, ^{13}C NMR spectra were recorded on a Bruker Avance 500 NMR spectrometer. All chemical shifts are reported in ppm with residual solvents or TMS (tetramethylsilane) as the internal standards. Fluorescence spectra (FL) were obtained on a Hitachi F-7100 fluorescence spectrophotometer. UV-vis spectra (UV) were obtained on a Shimadzu UV-2600i spectrometer. Scanning electron microscope (SEM) was tested by Phenom XL. HPLC data were obtained by Waters E2695. The synthesis of water soluble tetralactam macrocycle **H1** has been reported earlier.[1]

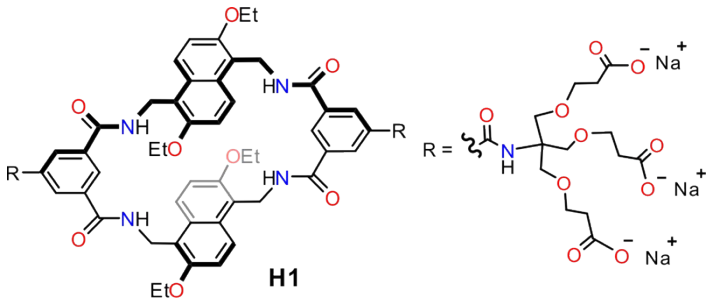

1.2 UV-vis Titrations

For UV-vis titrations, a 1.0×10^{-5}~2.5×10^{-5} M solution of the guest was prepared in PB buffer (10 mM, pH = 7.4, 25 °C) and a 0.8×10^{-3}~5×10^{-3} M solution of the host was prepared by using the prepared guest solution. The guest solution was placed in a cuvette (2 mL) at 25 °C. The solution of the host was then titrated until the UV absorbance did not change. The maximum change in absorbance was calculated from the theoretical fit at complete 1:1 binding isotherm was assumed for all titrations. Nonlinear curve-fitting method was then used to obtain the association constant through the following equation:

$$A=A_0+(((A-A_0)/2)/G_0)*(G_0+H+1/K_a-sqrt((G_0+H+1/K_a)\text{^}2-4*G_0*H))$$

All of these UV-vis titration experiments have been repeated three times. Errors are smaller than ± 10%.

1.3 Fluorescence Titrations

For fluorescence titrations, a 2.0×10^{-6}~2.5×10^{-5} M solution of the guest was prepared in PB buffer (10 mM, pH = 7.4, 25 °C) and a 1.0×10^{-3}~2.5×10^{-3} M solution of the host was prepared by using the prepared guest solution. The guest solution was placed in a cuvette (2 mL) at 25 °C. The solution of the host was then titrated until the fluorescence intensity did not change. The maximum change in fluorescence was calculated from the theoretical fit at complete 1:1 binding isotherm was assumed for all titrations. Nonlinear curve-fitting method was then used to obtain the association constant through the following equation:

$$I=I_0+(((I-I_0)/2)/G_0)*(G_0+H+1/K_a-sqrt((G_0+H+1/K_a)\text{^}2-4*G_0*H))$$

All of these fluorescence titration experiments have been repeated three times. Errors are smaller than ± 10%.

To get the binding constants of **UA**, we also used the competitive titration method.[2] The calibration lines were established at 25 °C in the intensity of the fluorescence responses of **RF@H1** reporter pair upon gradual titration of **UA** in PB buffer solution (10 mM, pH = 7.4). The fitting module for competitive titration was downloaded from the website of Prof. Nau's group. Accordingly, the increase in fluorescence intensity (I) by displacement of **RF** with varying competitor concentration follows:

$$I/I_0=I_{max}+([H_0](I_{rel}-I_{max}))/(K_{\mathbf{RF}}+[H_0])$$

Where I_0 is the fluorescence intensity in the absence of competition, I_{max} is the fluorescence intensity of **RF** at quantitative displacement, and I_{rel} is the relative fluorescence intensity of complexed **RF**. $K_{\mathbf{RF}}$ is the known binding constant of the complex and $[H_0]$ is the concentration of uncomplexed **H1**. All experiments were carried out in PB buffer solution (10 mM, pH = 7.4) at 25 °C. All of these fluorescence titration experiments have been repeated three times. Errors are smaller than ± 10%.

1.4 High Performance Liquid Chromatography (HPLC)

1.4.1 Preparation of standard solution

The uric acid was dissolved in PB buffer (10 mM, pH = 7.4), prepared into 0.5 mM and stored at 4 ℃. Appropriate amount of 0.5 mM uric acid standard solution was obtained by a micropipette. Then, it was diluted with PB buffer (10 mM, pH = 7.4), to prepare a series of standard solutions of 10, 25, 50, 100, 150, 200, 300, 400, 500 μM successively.

1.4.2 Pretreatment of real urine samples

200 μL urine sample was taken into a 5 mL centrifuge tube, added with 1800 μL PB buffer (10 mM, pH = 7.4), ultrasonic for 10 min, centrifuge at 4000 r/min for 8 min, the supernatant was taken through 0.22 μm microporous filter membrane for later use.

1.4.3 Detection by HPLC

All urine samples were preliminarily determined by HPLC. In this study, methanol: 3% phosphoric acid aqueous solution = 70:30 was used as the mobile phase. Symmetry C18 Column was used to analyze the urine samples, and the uric acid separation effect was good. The injection volume and time were 20 μL and 10 min respectively, and the flow rate was 0.7 mL/min.

2. NMR Spectra of Host-Guest Complexes

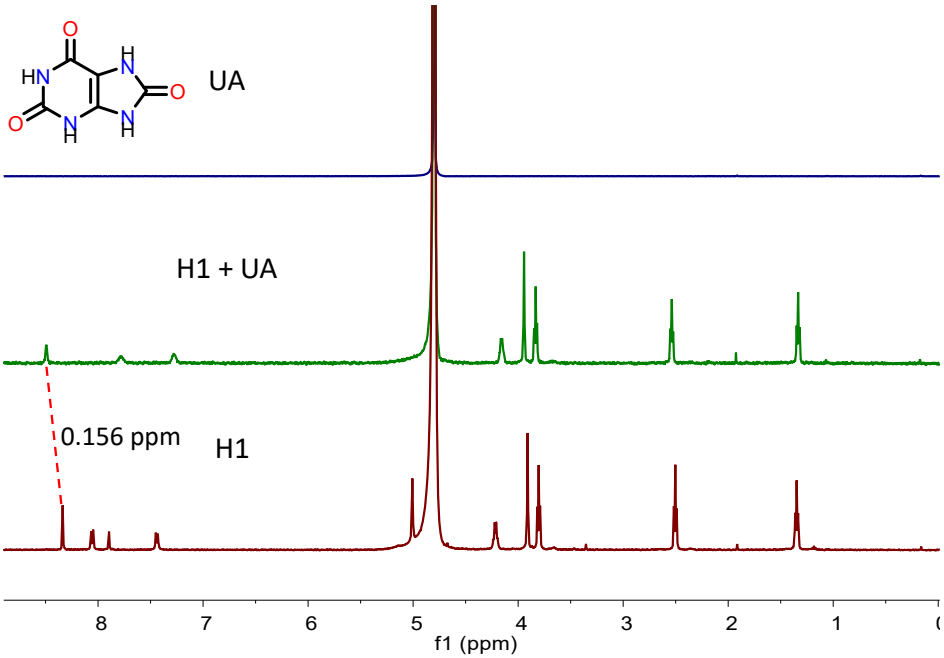

Fig. S1. ^{1}H NMR spectra (500 MHz, D_2O, 298 K) of uric acid (**UA**), **H1** (0.25 mM), and its equimolar mixture. The proton of the guest experiences the upfield shift, suggesting that the complexation between **H1** and guest **UA**.

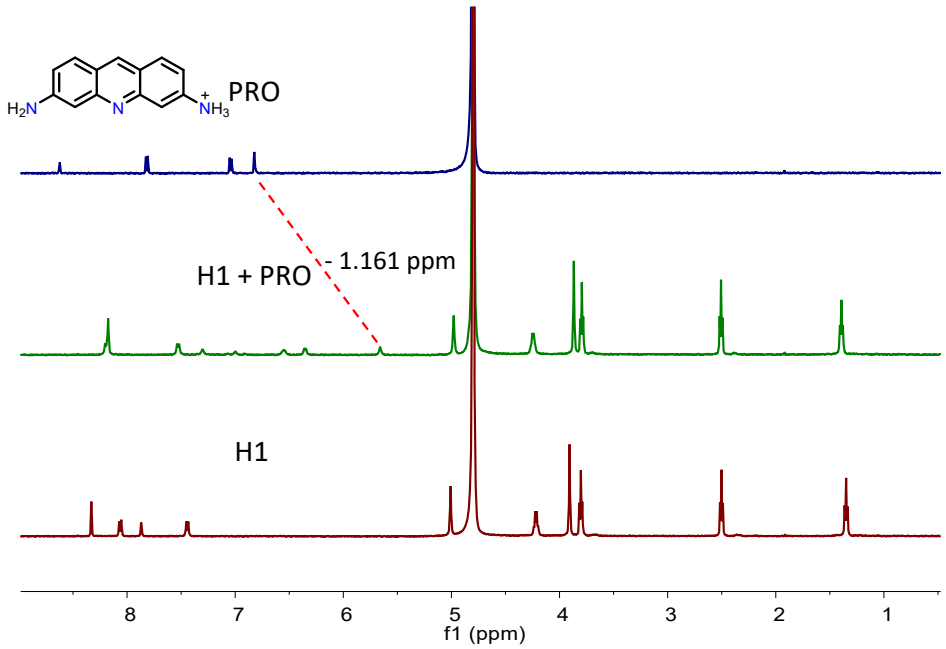

Fig. S2. ^{1}H NMR spectra (500 MHz, D_2O, 298 K) of **Proflavine**, **H1** (0.25 mM), and its equimolar mixture. The proton of the guest experiences the upfield shift, suggesting that the complexation between **H1** and guest **Proflavine**.

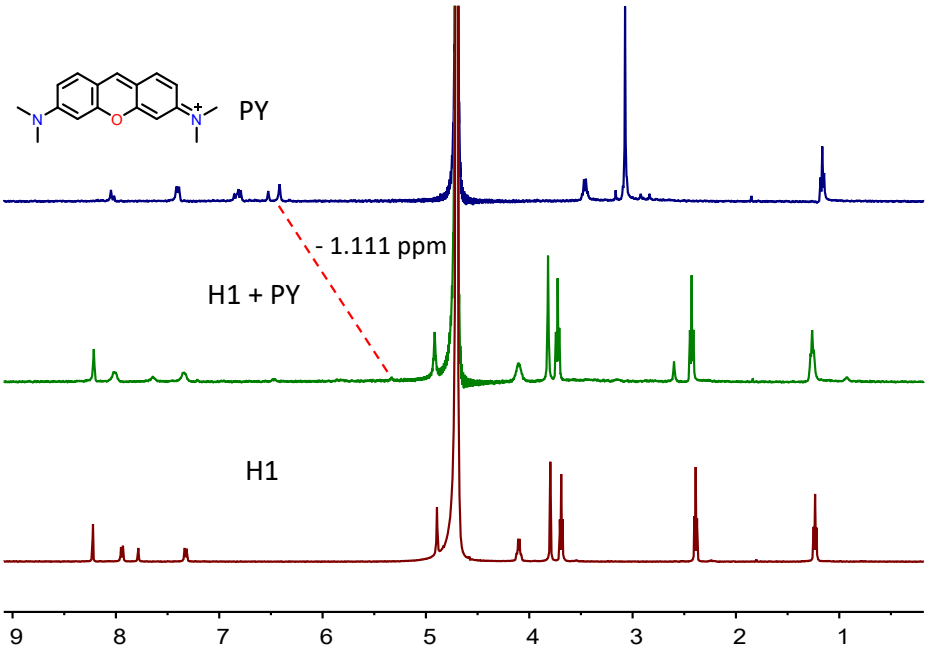

Fig. S3. ^{1}H NMR spectra (500 MHz, D_2O, 298 K) of **Pyronin Y**, **H1** (0.25 mM), and its equimolar mixture. The proton of the guest experiences the upfield shift, suggesting that the complexation between **H1** and guest **Pyronin Y**.

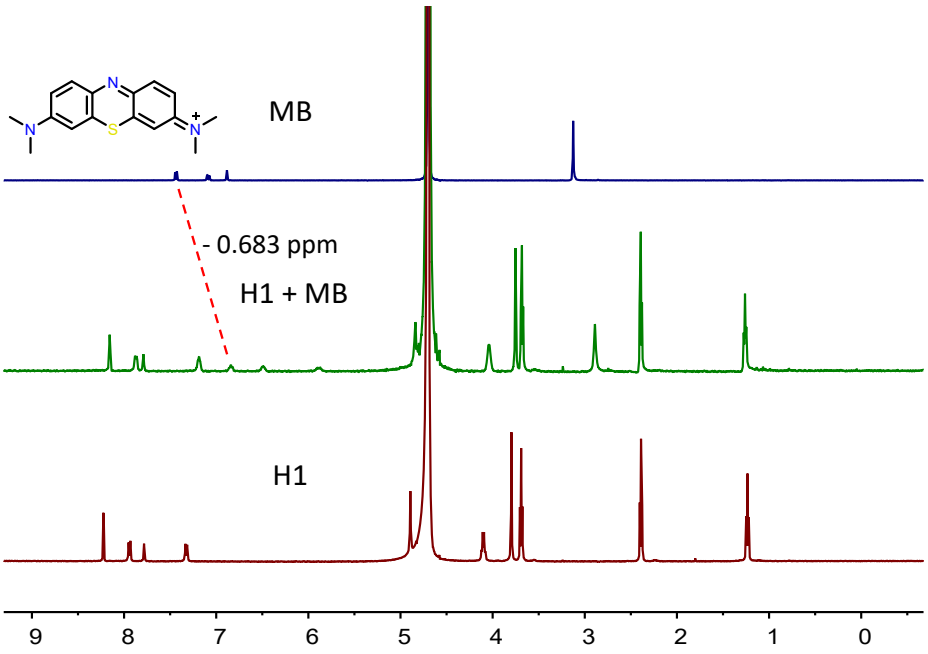

Fig. S4. ^{1}H NMR spectra (500 MHz, D_2O, 298 K) of **Methylene Blue**, **H1** (0.25 mM), and its equimolar mixture. The proton of the guest experiences the upfield shift, suggesting that the complexation between **H1** and guest **Methylene Blue**.

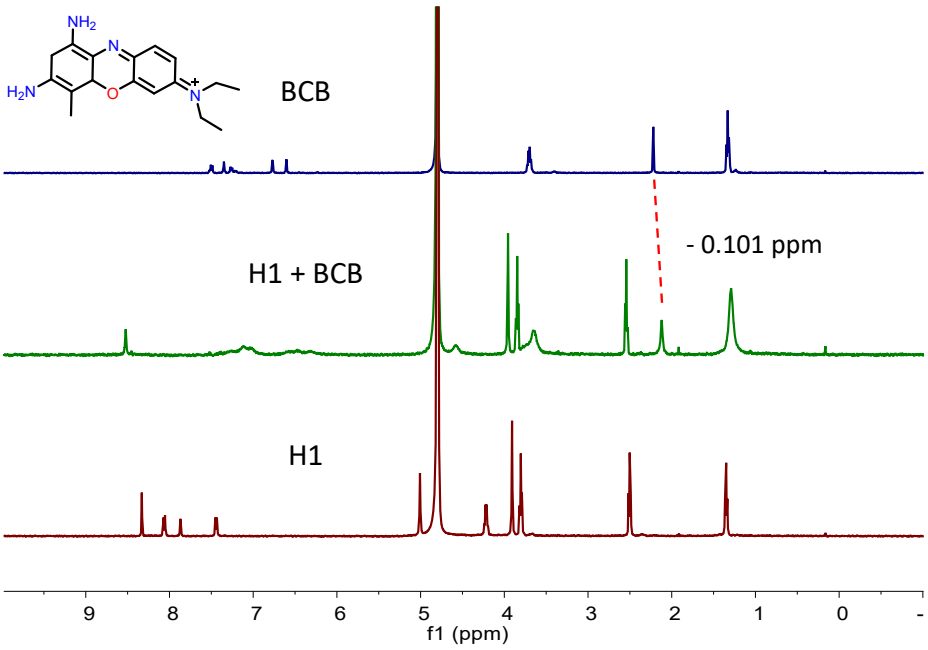

Fig. S5. ^{1}H NMR spectra (500 MHz, D_2O, 298 K) of **Brilliant Cresyl Blue**, **H1** (0.25 mM), and its equimolar mixture. The proton of the guest experiences the upfield shift, suggesting that the complexation between **H1** and guest **Brilliant Cresyl Blue**.

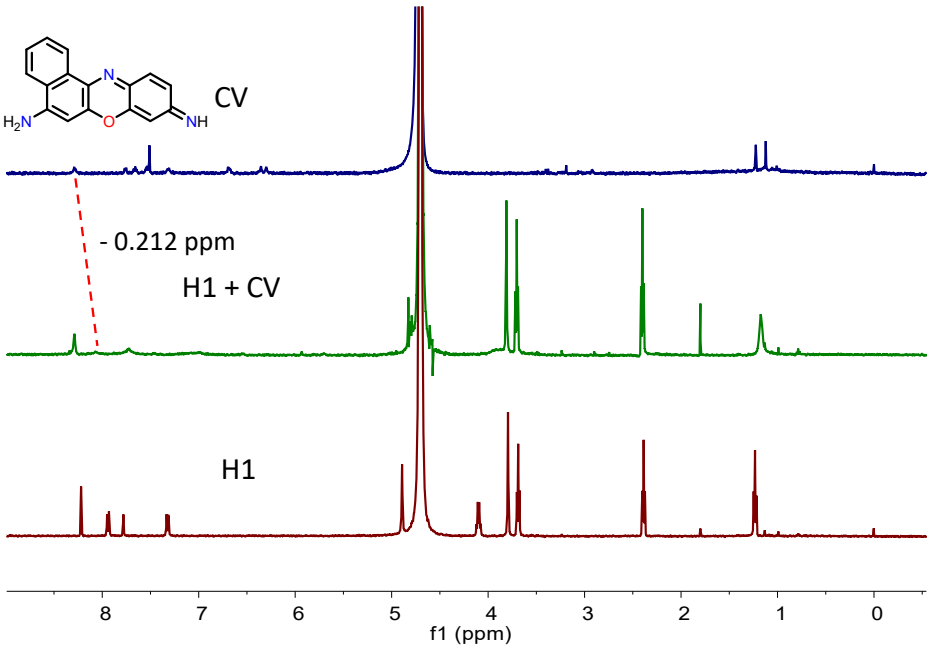

Fig. S6. ^{1}H NMR spectra (500 MHz, D_2O, 298 K) of **Cresyl Violet**, **H1** (0.25 mM), and its equimolar mixture. The proton of the guest experiences the upfield shift, suggesting that the complexation between **H1** and guest **Cresyl Violet**.

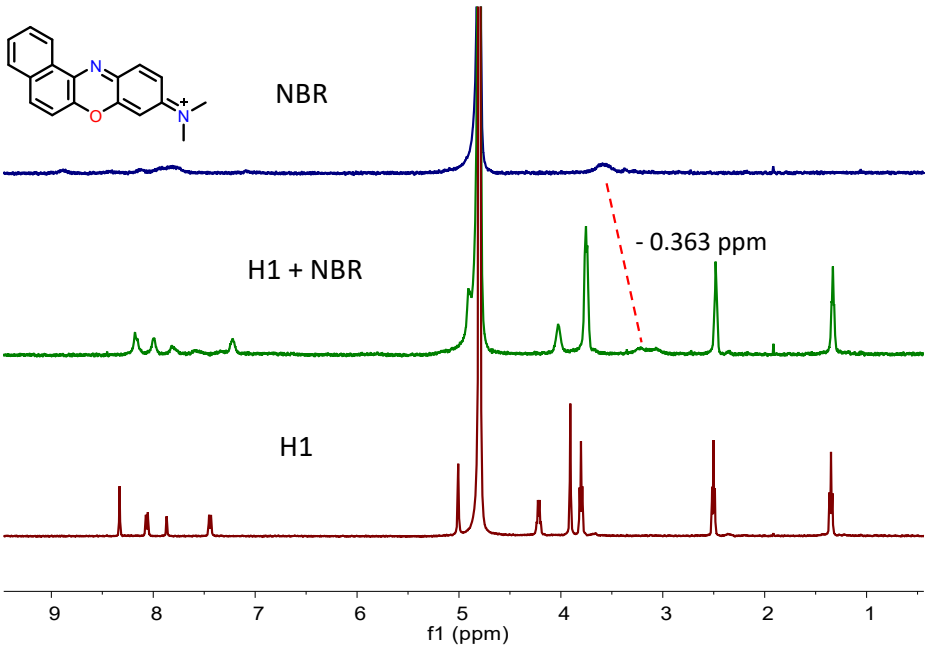

Fig. S7. ^{1}H NMR spectra (500 MHz, D_2O, 298 K) of **Medola's Blue**, **H1** (0.25 mM), and its equimolar mixture. The proton of the guest experiences the upfield shift, suggesting that the complexation between **H1** and guest **Medola's Blue**.

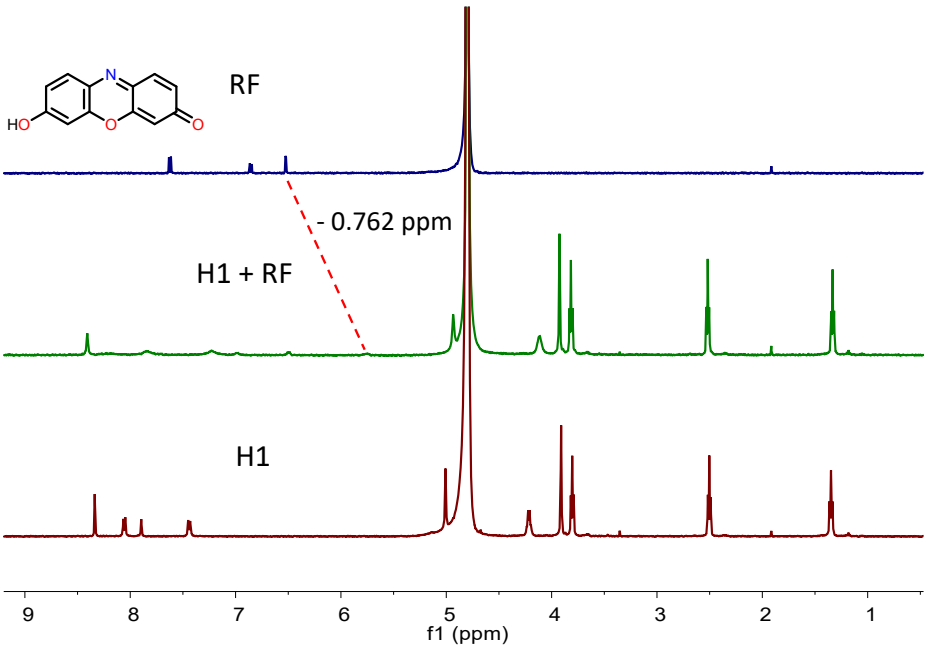

Fig. S8. ^{1}H NMR spectra (500 MHz, D_2O, 298 K) of **Resorufin**, **H1** (0.25 mM), and its equimolar mixture. The proton of the guest experiences the upfield shift, suggesting that the complexation between **H1** and guest **Resorufin**.

3. Determination of Binding Parameters

All of these UV-vis and fluorescence titration experiments have been repeated three times, and the average values and standard deviations are given in Table S1. Errors are smaller than ± 10%. The following is the figure of one of three repeated experiments.

Table S1. Binding constants (K_a) of dyes with H1 as determined by UV-vis, fluorescence (FL), and ITC titrations (PB buffer, 10 mM, pH 7.4) at 25 °C.

Dye	K_a (M^{-1})		
	UV-vis	FL	ITC
PRO	$(1.85 \pm 0.12) \times 10^4$	$(2.76 \pm 0.25) \times 10^4$	-
PY	$(1.91 \pm 0.04) \times 10^5$	$(2.15 \pm 0.19) \times 10^5$	-
RFN[a]	-	-	1.2×10^7
MB	$(3.98 \pm 0.19) \times 10^5$	$(4.45 \pm 0.33) \times 10^5$	-
RF	$(4.63 \pm 0.15) \times 10^4$	$(3.83 \pm 0.20) \times 10^4$	-
BCB	$(4.62 \pm 0.17) \times 10^4$	$(6.43 \pm 0.58) \times 10^4$	-
CV	-[b]	$(8.49 \pm 0.23) \times 10^5$	-
NBR	$(4.97 \pm 0.27) \times 10^4$	$(8.70 \pm 0.08) \times 10^4$	-

[a] Value was taken from ref 1; [b] The binding constant was too large to fit accurately.

3.1 UV-vis Titrations

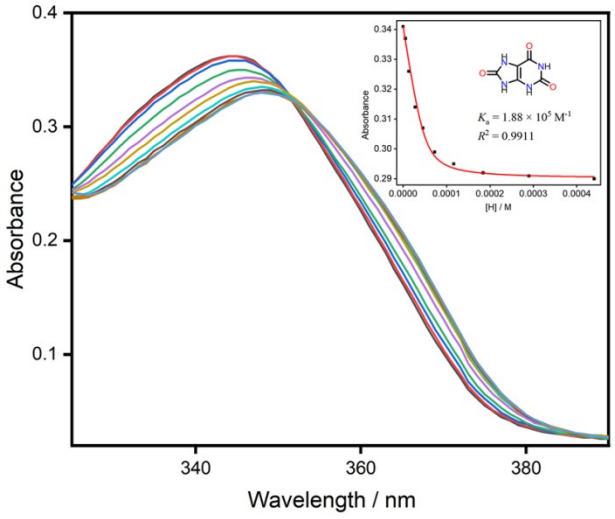

	K_a (M^{-1})	R^2
1 st	1.88×10^5	0.9911
2 nd	1.51×10^5	0.9977
3 rd	1.74×10^5	0.9954
average	$(1.70 \pm 0.18) \times 10^5$	

Fig. S9. UV-vis titration of compound **H1** with **UA** in PB buffer (10 mM, pH = 7.4, [G] = 3.7 mM; [**H1**] = 50 μM). Fit of the titration data at λ_{ab} = 344 nm to a single-site binding isotherm

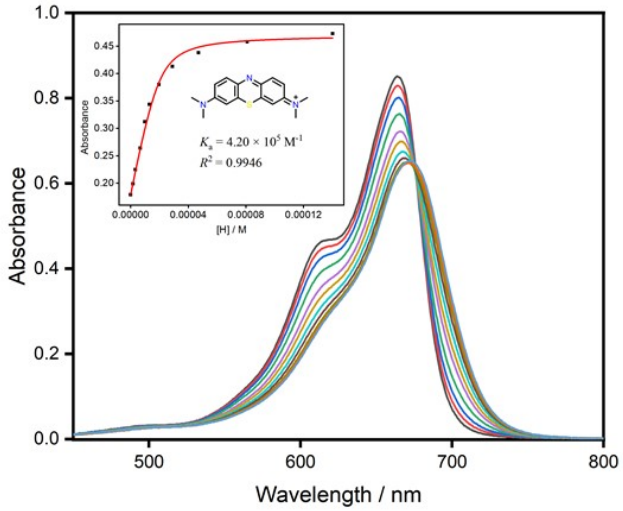

	K_a (M^{-1})	R^2
1 st	4.20×10^5	0.9946
2 nd	3.85×10^5	0.9965
3 rd	3.89×10^5	0.9973
average	$(3.98 \pm 0.19) \times 10^5$	

Fig. S10. UV-vis titration of compound **Methlene Blue** with **H1** in PB buffer (10 mM, pH = 7.4, [G] = 20 μM; [**H1**] = 0.8 mM). Fit of the titration data at λ_{ab} = 691 nm to a single-site binding isotherm.

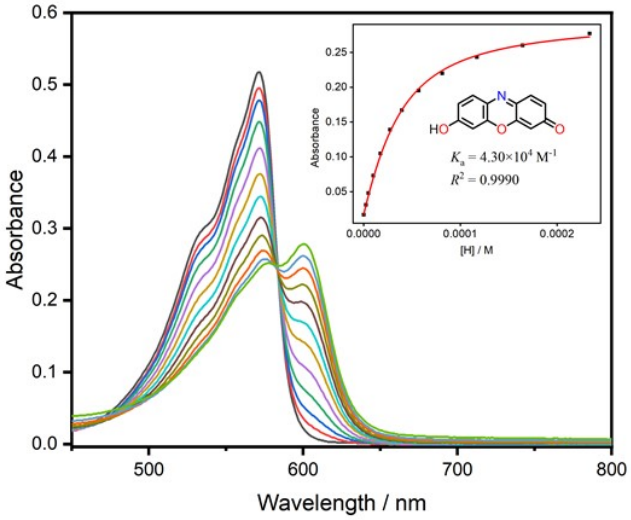

	K_a (M^{-1})	R^2
1 st	4.30×10^4	0.9990
2 nd	3.94×10^4	0.9980
3 rd	4.01×10^4	0.9980
average	$(4.08 \pm 0.19) \times 10^4$	

Fig. S11. UV-vis titration of compound **Resorufin** with **H1** in PB buffer (10 mM, pH = 7.4, [G] = 25 μM; [**H1**] = 5 mM). Fit of the titration data at λ_{ab} = 602 nm to a single-site binding isotherm.

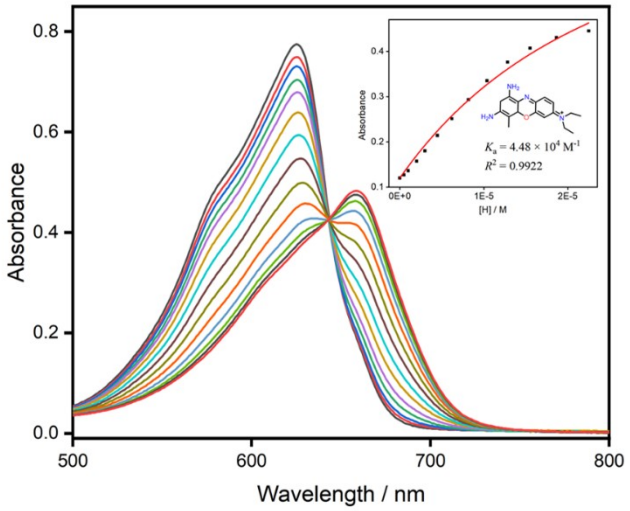

	K_a (M^{-1})	R^2
1 st	4.48×10^4	0.9922
2 nd	4.80×10^4	0.9991
3 rd	4.56×10^4	0.9917
average	$(4.08 \pm 0.19) \times 10^4$	

Fig. S12. UV-vis titration of compound **Brilliant Cresyl Blue** with **H1** in PB buffer (10 mM, pH = 7.4, [G] = 5 μM; [**H1**] = 1 mM). Fit of the titration data at λ_{ab} = 666 nm to a single-site binding isotherm.

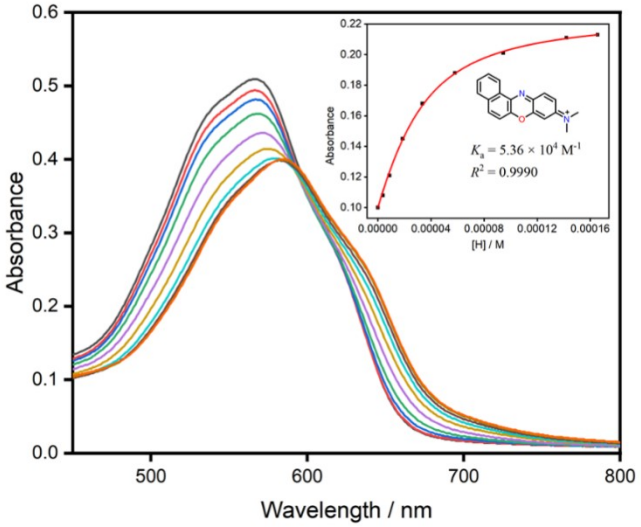

	K_a (M^{-1})	R^2
1 st	5.36×10^4	0.9990
2 nd	4.76×10^4	0.9995
3 rd	4.81×10^4	0.9993
average	$(4.97 \pm 0.27) \times 10^4$	

Fig. S13. UV-vis titration of compound **Meldola's Blue** with **H1** in PB buffer (10 mM, pH = 7.4, [G] = 5 μM; [**H1**] = 1 mM). Fit of the titration data at λ_{ab} = 666 nm to a single-site binding isotherm.

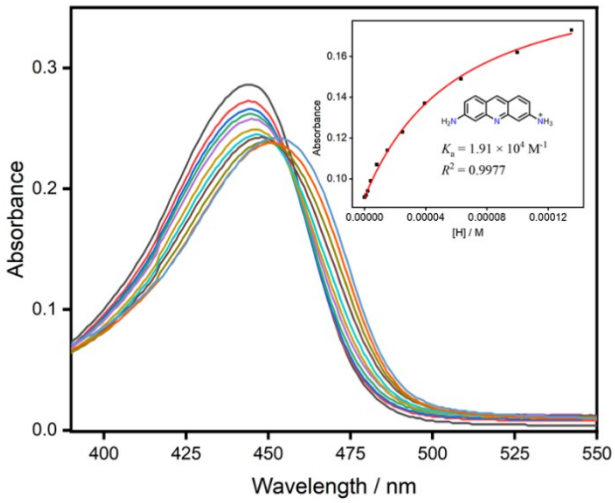

	K_a (M^{-1})	R^2
1 st	1.91×10^4	0.9977
2 nd	1.92×10^4	0.9988
3 rd	1.71×10^4	0.9958
average	$(1.85 \pm 0.12) \times 10^4$	

Fig. S14. UV-vis titration of compound **Proflavin** with **H1** in PB buffer (10 mM, pH = 7.4, [G] = 10 μM; [**H1**] = 5 mM). Fit of the titration data at λ_{ab} = 470 nm to a single-site binding isotherm.

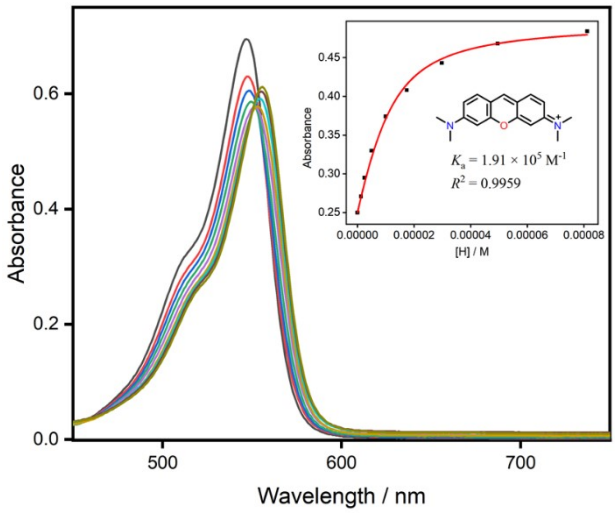

	K_a (M^{-1})	R^2
1 st	1.91×10^5	0.9959
2 nd	1.87×10^5	0.9908
3 rd	1.94×10^5	0.9931
average	$(1.91 \pm 0.04) \times 10^5$	

Fig. S15. UV-vis titration of compound **Pyronin Y** with **H1** in PB buffer (10 mM, pH = 7.4, [G] = 10 μM; [**H1**] = 5 mM). Fit of the titration data at λ_{ab} = 564 nm to a single-site binding isotherm.

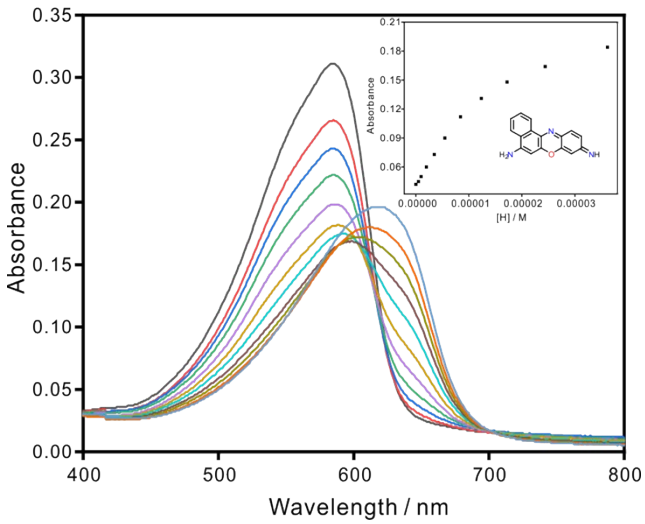

Fig. S16. UV-vis titration of compound **Cresyl Violet** with **H1** in PB buffer (10 mM, pH = 7.4, [G] = 10 μM; [**H1**] = 5 mM). The binding constant was too large to fit accurately.

3.2 Fluorescence Titrations

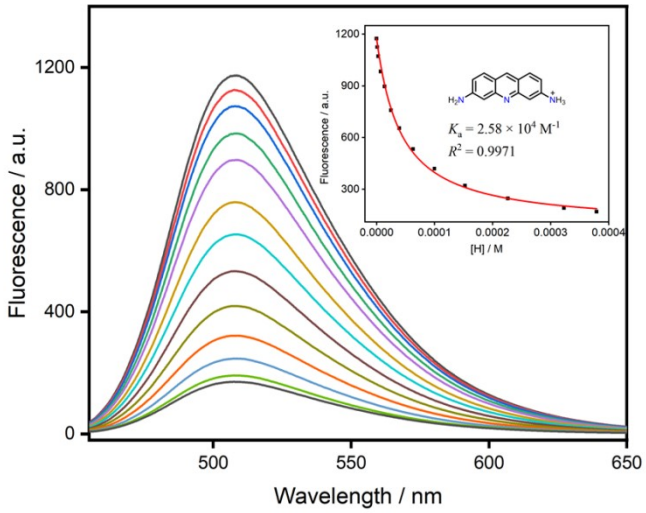

	K_a (M^{-1})	R^2
1 st	2.58×10^4	0.9971
2 nd	2.65×10^4	0.9977
3 rd	3.05×10^4	0.9987
average	$(2.76 \pm 0.25) \times 10^4$	

Fig. S17. Fluorescence titration of compound **Proflavine** with **H1** in PB buffer (10 mM, pH = 7.4, [G] = 5 μM; [**H1**] = 2 mM). Fit of the titration data at λ_{em} = 509 nm to a single-site binding isotherm.

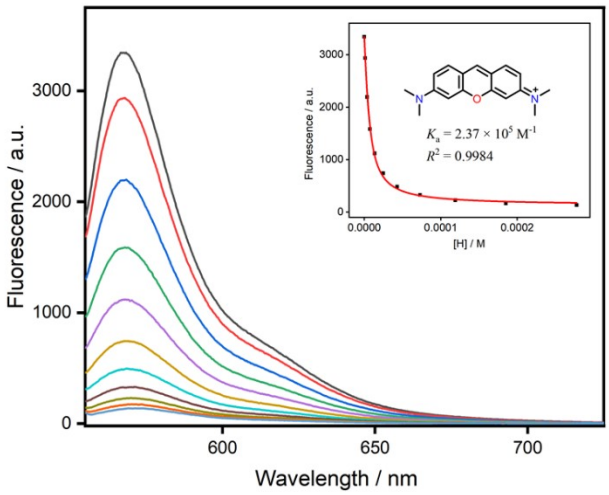

	K_a (M^{-1})	R^2
1 st	2.37×10^5	0.9984
2 nd	2.02×10^5	0.9967
3 rd	2.07×10^5	0.9971
average	$(2.15 \pm 0.19) \times 10^4$	

Fig. S18. Fluorescence titration of compound **Pyronin Y** with **H1** in PB buffer (10 mM, pH = 7.4, [G] = 5 μM; [**H1**] = 2.5 mM). Fit of the titration data at λ_{em} = 568 nm to a single-site binding isotherm.

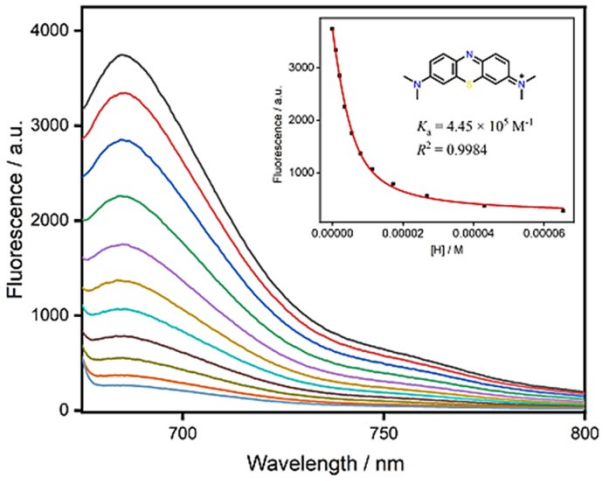

	K_a (M^{-1})	R^2
1 st	4.45×10^5	0.9984
2 nd	4.05×10^5	0.9974
3 rd	4.85×10^5	0.9976
average	$(4.45 \pm 0.33) \times 10^5$	

Fig. S19. Fluorescence titration of compound **Methylene Blue** with **H1** in PB buffer (10 mM, pH = 7.4, [G] = 5 μM; [**H1**] = 1 mM). Fit of the titration data at λ_{em} = 685 nm to a single-site binding isotherm.

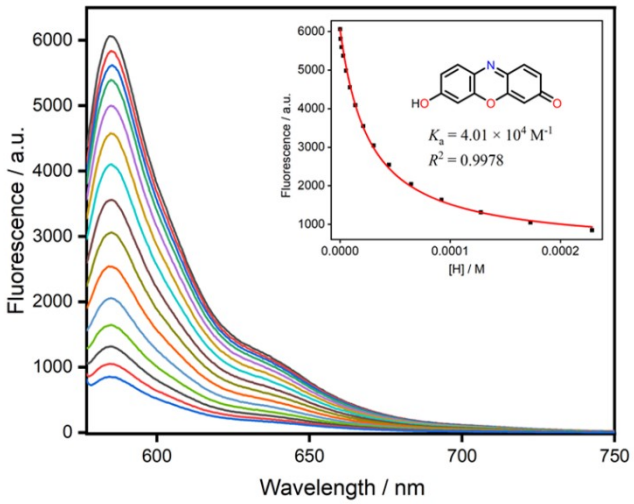

	K_a (M^{-1})	R^2
1 st	4.01×10^4	0.9978
2 nd	3.61×10^4	0.9995
3 rd	3.86×10^4	0.9976
average	$(3.82 \pm 0.20) \times 10^4$	

Fig. S20. Fluorescence titration of compound **Resorufin** with **H1** in PB buffer (10 mM, pH = 7.4, [G] = 2 μM; [**H1**] = 2.5 mM). Fit of the titration data at λ_{em} = 586 nm to a single-site binding isotherm.

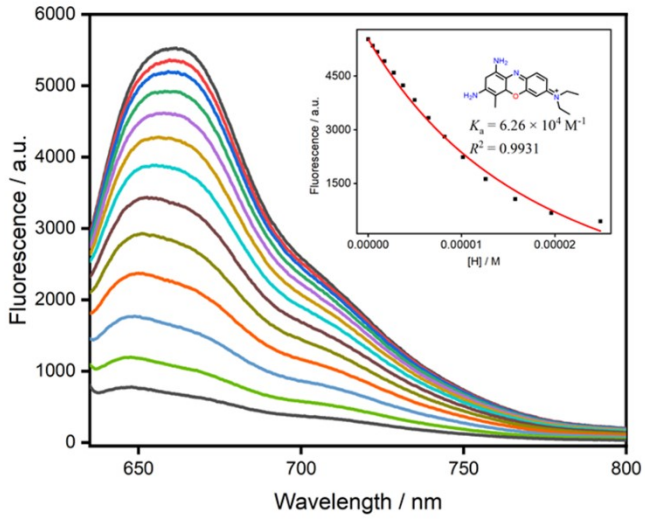

	K_a (M^{-1})	R^2
1 st	6.26×10^4	0.9931
2 nd	7.07×10^4	0.9924
3 rd	5.94×10^4	0.9900
average	$(6.43 \pm 0.58) \times 10^4$	

Fig. S21. Fluorescence titration of compound **Brilliant Cresyl Blue** with **H1** in PB buffer (10 mM, pH = 7.4, [G] = 5 μM; [**H1**] = 1 mM). Fit of the titration data at λ_{em} = 663 nm to a single-site binding isotherm.

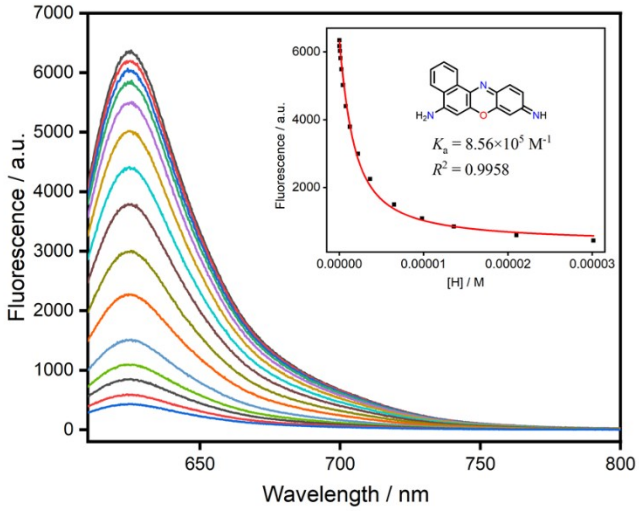

	K_a (M^{-1})	R^2
1 st	8.56×10^5	0.9958
2 nd	8.75×10^5	0.9956
3 rd	8.29×10^5	0.9955
average	$(8.58 \pm 0.15) \times 10^5$	

Fig. S22. Fluorescence titration of compound **Cresyl Violet** with **H1** in PB buffer (10 mM, pH = 7.4, [G] = 1 μM; [**H1**] = 1 mM). Fit of the titration data at λ_{em} = 624 nm to a single-site binding isotherm.

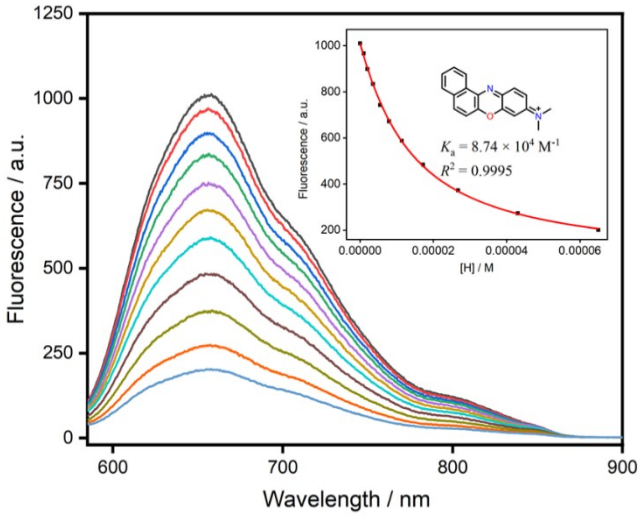

	K_a (M^{-1})	R^2
1 st	8.74×10^4	0.9995
2 nd	8.61×10^4	0.9989
3 rd	8.75×10^4	0.9998
average	$(8.70 \pm 0.08) \times 10^4$	

Fig. S23. Fluorescence titration of compound **Meldola's Blue** with **H1** in PB buffer (10 mM, pH = 7.4, [G] = 5 μM; [**H1**] = 1 mM). Fit of the titration data at λ_{em} = 655 nm to a single-site binding isotherm.

4. Computational Host-Guest Complex Structures

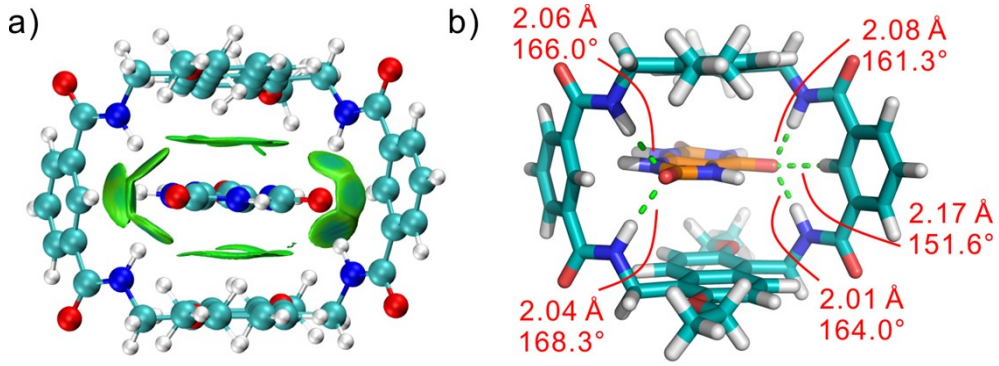

Fig. S24. Energy-minimized structures and IGMH (δg_{inter} = 0.005) analysis of **UA@H1** obtained by DFT (ωB97XD/6-31G(d,p)) calculations with the SMD solution model in water.

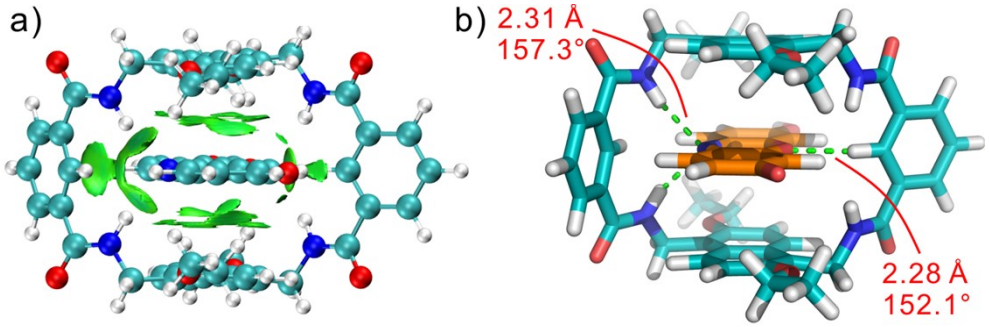

Fig. S25. Energy-minimized structures and IGMH (δg_{inter} = 0.005) analysis of **RF@H1** obtained by DFT (ωB97XD/6-31G(d,p)) calculations with the SMD solution model in water.

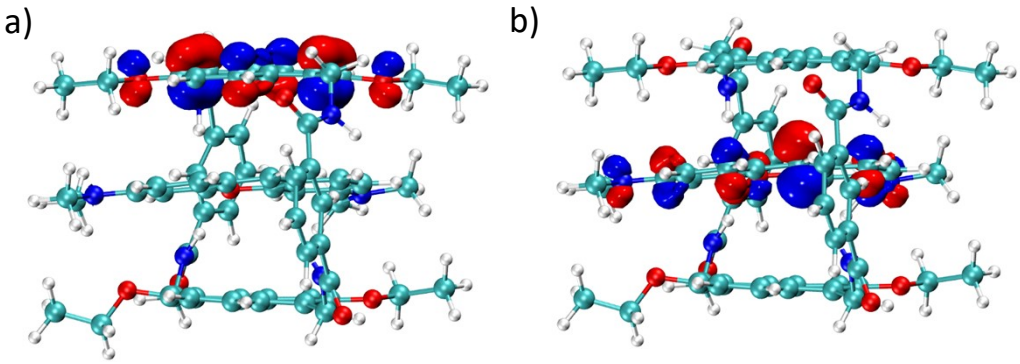

Fig. S26. DFT calculated a) HOMO and b) LUMO orbitals of **PY@H1** (energy gap: 5.72 eV).

5. The Detection of Uric Acid

Table S2. Changes in UV absorption and fluorescence intensity of dyes at the

titration of H1 or UA.

Dye	+ **H1**		**UA** response (%)[c]	I_1/I^d
	Δ (nm)[a]	I/I_0[b]		
Proflavine	10	0.3	41	1.4
Pyronin Y	9	0.1	46	4.6
Riboflavin	11	0.1	25	2.5
Methylene Blue	8	0.1	36	3.6
Resorufin	30	0.1	94	9.4
Brilliant Cresyl Blue	35	0.1	39	3.9
Cresyl Violet	35	0.1	47	4.7
Meldola's Blue	20	0.2	32	1.6

[a)] The red shift value of the dye in UV-vis spectra after the addition of saturated macrocycle **H1**. [b)] I_0 and I are the fluorescence intensities of the dye before and after addition of **H1**. [c)] The fluorescence intensity recovery percentage of dye@**H1** compared to dye upon adding saturated **UA**. [d)] I and I_1 are the fluorescence intensities of dye@**H1** before and after addition of **UA**.

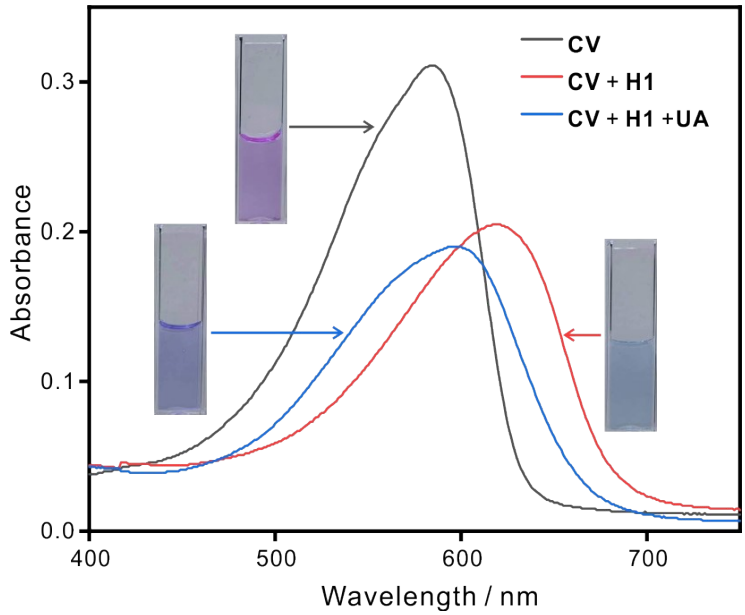

Fig. S27. UV-vis absorption spectra of **CV**, **CV** + **H1**, and **CV** + **H1** + **UA**. 10 mM PB buffer, pH 7.4, 25 °C, [**CV**] = 25 μM, [**H1**] = 20 μM, [**UA**] = 480 μM.

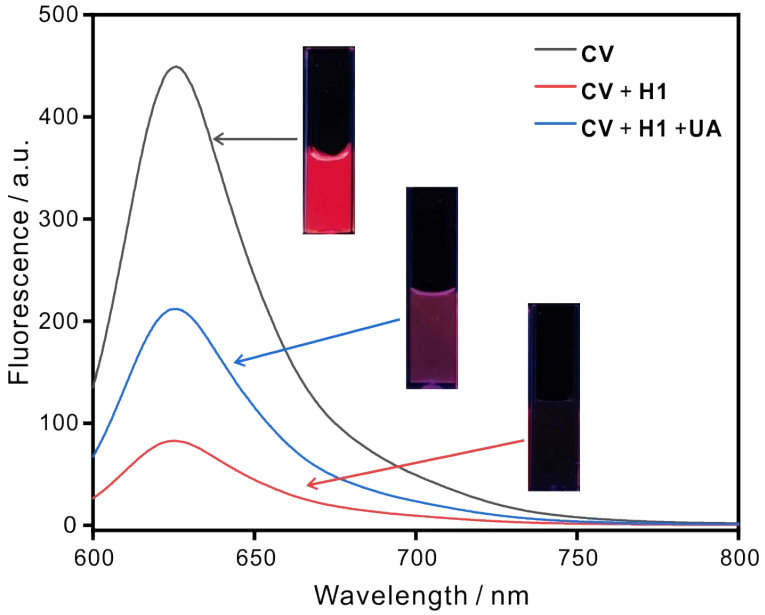

Fig. S28. Fluorescence spectra of **CV**, **CV** + **H1**, and **CV** + **H1** + **UA**. 10 mM PB buffer, pH 7.4, 25 °C, [**CV**] = 5 μM, [**H1**] = 10 μM, [**UA**] = 360 μM.

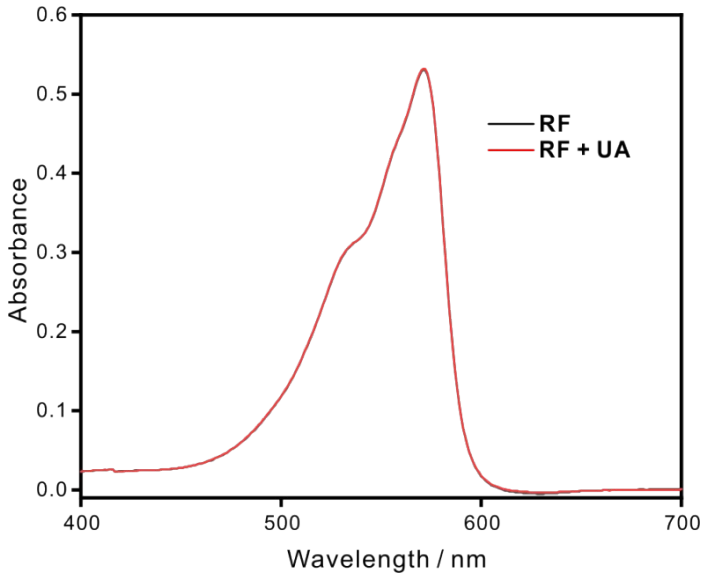

Fig. S29. UV-vis spectra of **RF**, **RF** with **UA**. 10 mM PB buffer, pH 7.4, 25 °C, [**RF**] = 10 μM, [**UA**] = 500 μM.

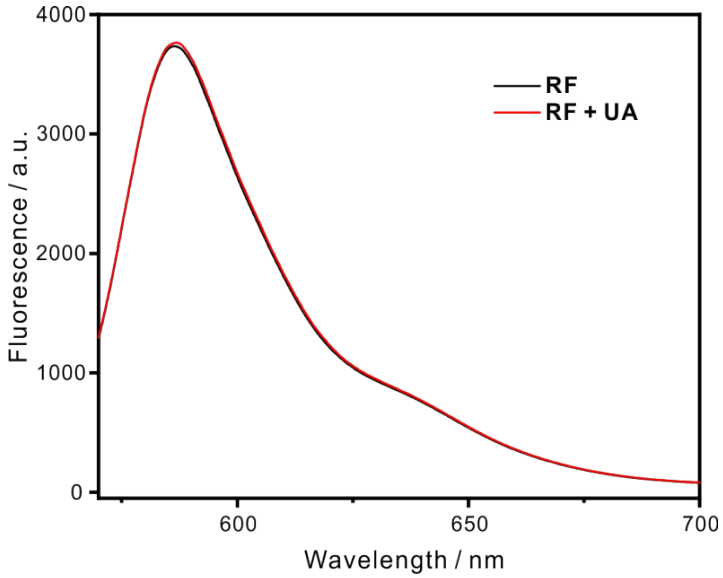

Fig. S30. Fluorescence spectra of **RF**, **RF** with **UA**. 10 mM PB buffer, pH 7.4, 25 °C, [**RF**] = 2 μM, [**UA**] = 100 μM.

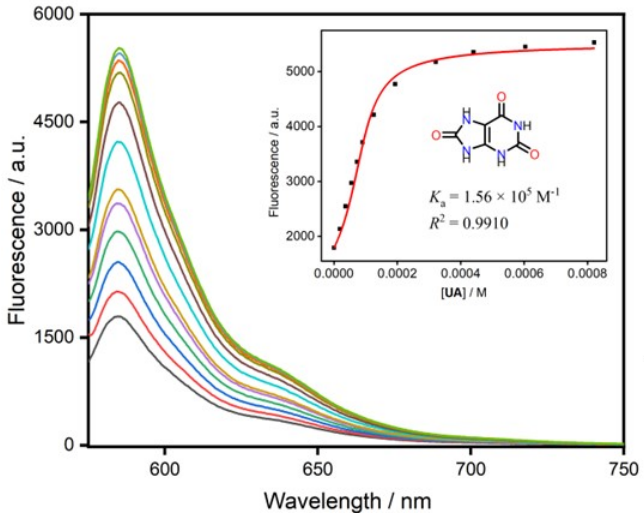

	K_a (M^{-1})	R^2
1 st	1.56 × 10^5	0.9910
2 nd	1.42 × 10^5	0.9913
3 rd	1.56× 10^5	0.9955
average	(1.51 ± 0.08) × 10^5	

Fig. S31. Competitive titration in the **RF@H1** (2 μM/90 μM) reporter pair performed with **UA** up to 0.8 mM in PB buffer (10 mM, pH = 7.4, 10 mM). Fit of the titration data at λ_{em} = 586 nm to a single-site binding isotherm.

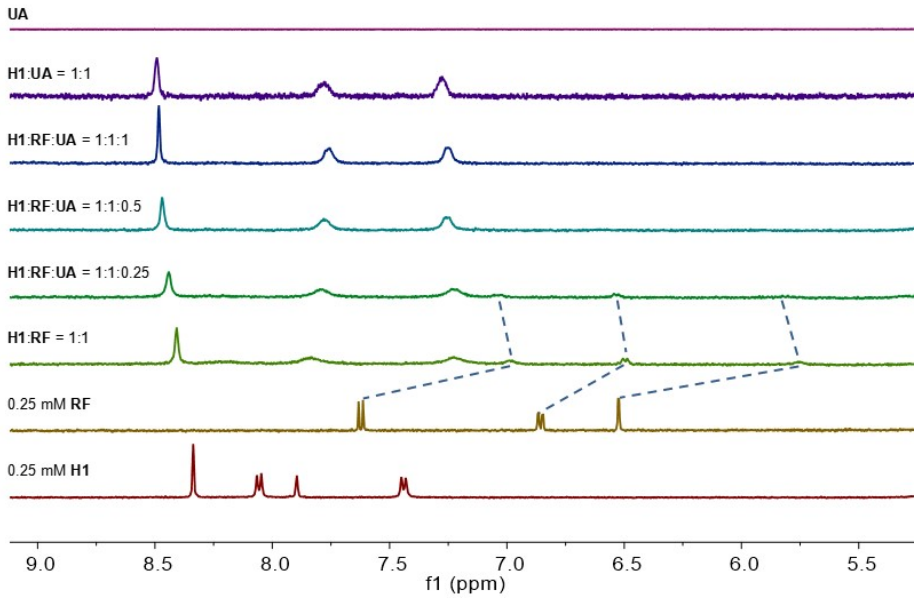

Fig. S32. Partial ^{1}H NMR spectra (500 MHz, D_2O, 25 ℃) of **H1**, **RF**, **UA**, the equimolar mixture of **H1** and **UA**, the equimolar mixture of **H1** and **RF** after gradually adding **UA**.

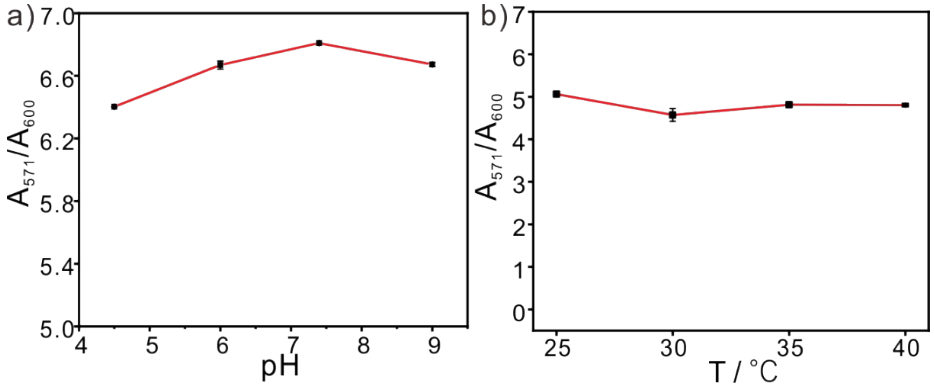

Fig. S33. Optimization of experimental parameters by UV. a) Effect of pH. **RF@H1** = 10/95 μM, **UA** = 134 μM, 25 ℃. b) Effect of temperature. **RF@H1** = 10/95 μM, **UA** = 134 μM, pH 7.4.

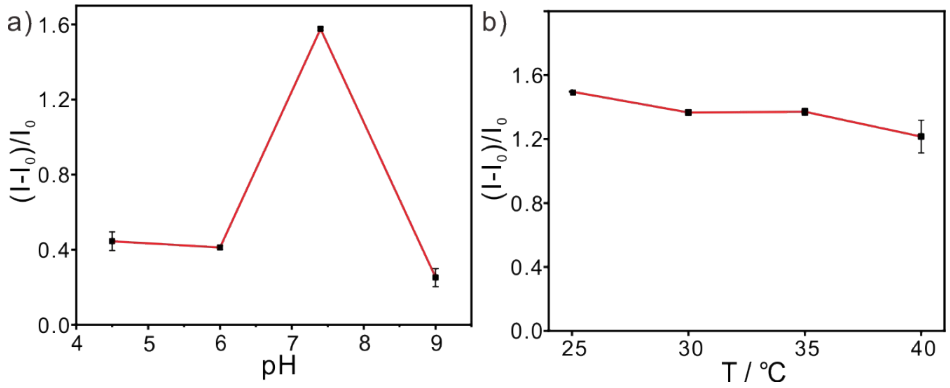

Fig. S34.Optimization of experimental parameters by Fluorescence. a) Effect of pH. **RF@H1** = 2/90 μM, **UA** = 90 μM, 25 ℃. b) Effect of temperature. **RF@H1** = 2/90 μM, **UA** = 90 μM, pH 7.4.

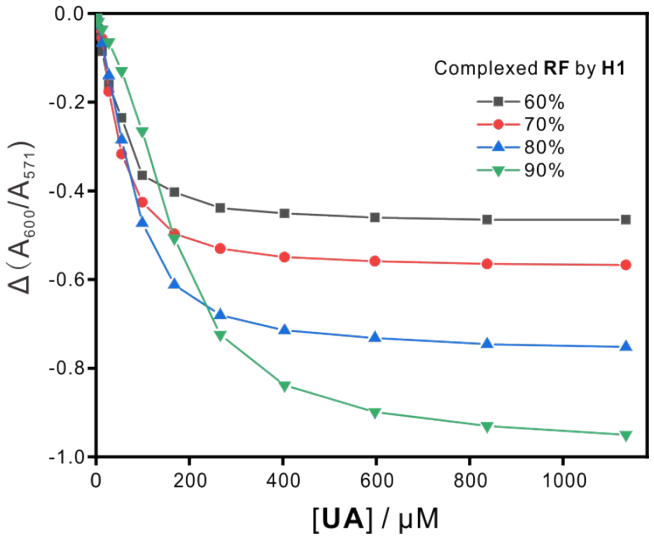

Fig. S35. The initial concentration of the indicator is $[\mathbf{RF}]_0$ =10 μM in each assay. The initial concentrations of the host are $[\mathbf{H1}]_0$ = 39 μM, 57 μM, 95 μM and 200 μM respectively, which correspond to the presence of 60%, 70%, 80% and 90% complexed **RF@H1**. **[RF]/[H1]** = 10 μM/95 μM was selected because of its strong response and high sensitivity.

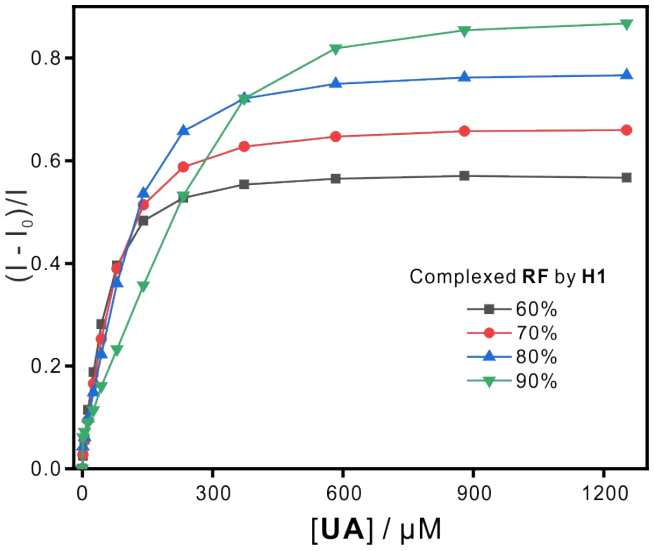

Fig. S36. Indicator displacement isotherms calculated from the binding constants $K_{\mathbf{RF\text{-}H1}}$= 4.0×10^4 M^{-1}. The initial concentration of the indicator is $[\mathbf{RF}]_0$ = 2 μM in each assay, the initial concentrations of the host are $[\mathbf{H1}]_0$ = 38 μM, 60 μM, 90 μM and 200 μM respectively, which correspond to the presence of 60%, 70%, 80% and 90% complexed **RF@H1**. **[RF]/[H1]** = 2 μM/90 μM was selected because of its strong response and high sensitivity.

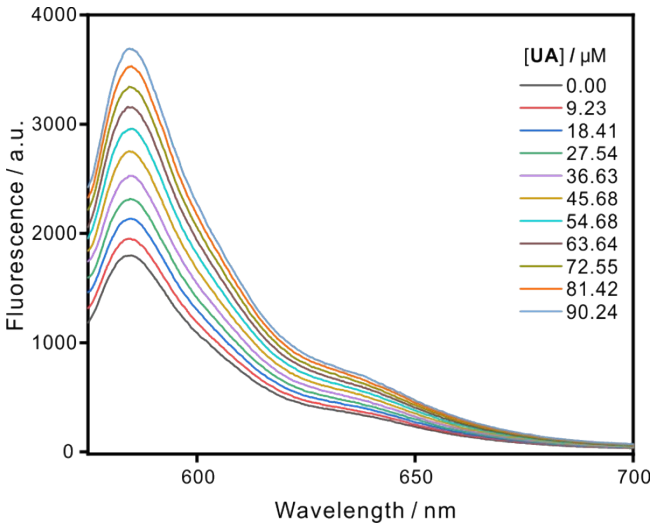

Fig. S37. Competitive titration in the **RF@H1** (2 μM/90 μM) reporter pair performed with **UA** up to 90.24 μM at λ_{ex} = 570 nm and λ_{em} = 586 nm.

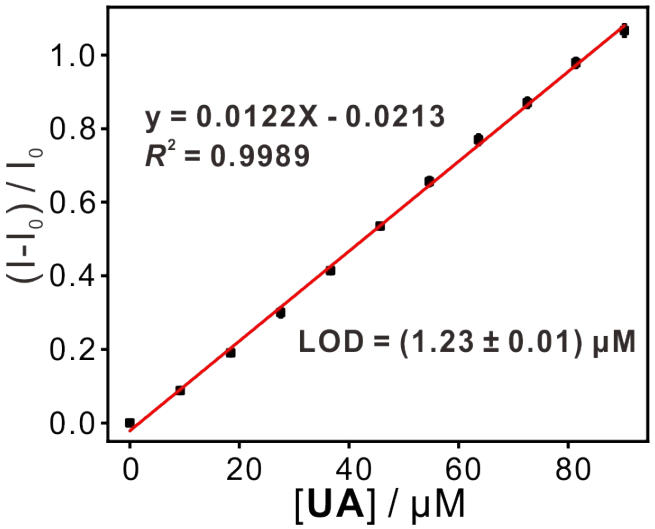

Fig. S38. The limit of detection (LOD) for **UA** in PB buffer solution (10 mM, pH = 7.4). The plot of $(I-I_0)/I_0$ against **UA** concentration in 10 mM PB buffer solution (10 mM, pH = 7.4, 25 ℃) with I_0 and I assigned as the fluorescence intensities of the **RF@H1** (2 μM/90 μM) reporter pair in the absence and presence of **UA** (0–90.24 μM) respectively.

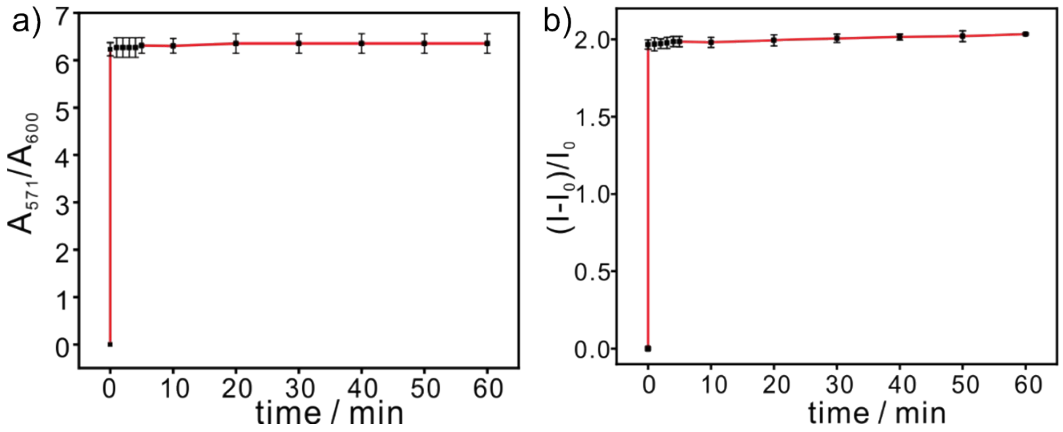

Fig. S39. a) UV and b) Fluorescence responses of the **RF@H1** (10 μM/95 μM and 2 μM/90 μM respectively) with time upon addition of **UA** (134 μM and 90 μM respectively). I_0 and I assigned as the fluorescence intensities of the **RF@H1** reporter pair in the absence and presence of **UA**. 10 mM PB buffer, pH 7.4, 25 ℃.

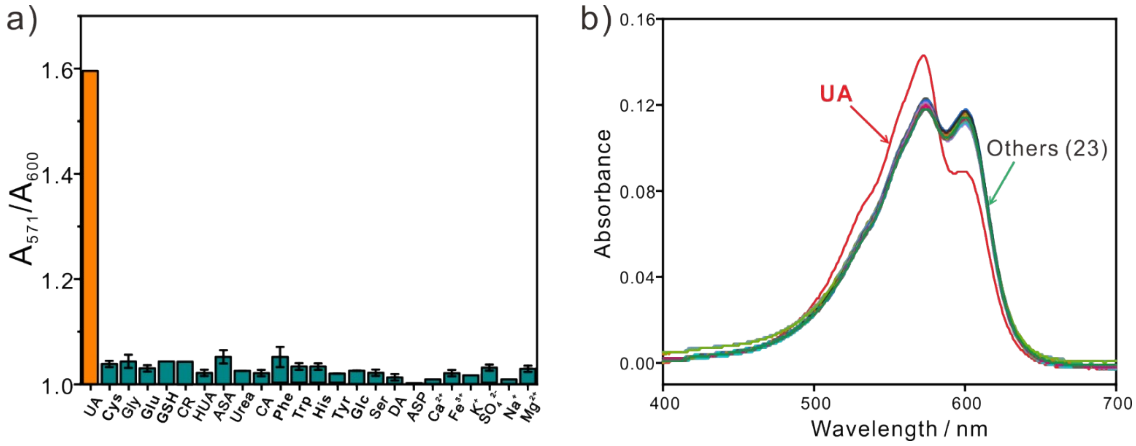

Fig. S40. UV responses of the **RF@H1** solution upon addition of **UA** or endogenous substances. 10 mM PB buffer, pH 7.4, 25 ℃, [**RF**] = 10 μM, [**H1**] = 95 μM, 50 μM for **UA**, **Cys**, **Gly**, **Glu**, **GSH**, **CR**, **HUA**, **ASA**, Urea, **CA**, **Phe**, **Trp**, **His**, **Tyr**, **Glc**, **Ser**, **DA**, **ASP**, 100 μM for Ca^{2+}, Fe^{3+}, K^+, SO_4^{2-}, Na^+ and Mg^{2+}, respectively.

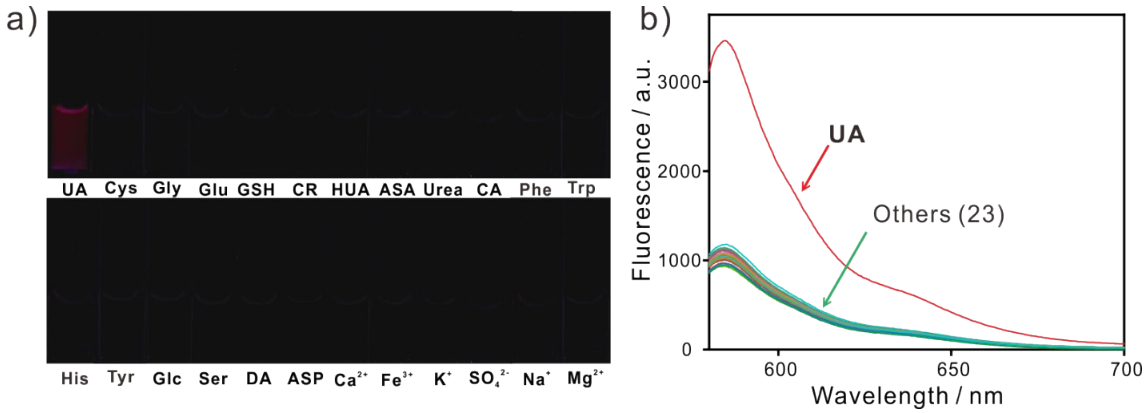

Fig. S41. a) the color change and b) Fluorescence responses of the **RF@H1** solution upon addition of **UA** or endogenous substances. 10 mM PB buffer, pH 7.4, 25 ℃, [**RF**] = 2 μM, [**H1**] = 90 μM, 0.4 mM for **UA**, **Cys**, **Gly**, **Glu**, **GSH**, **CR**, **HUA**, **ASA**, Urea, **CA**, **Phe**, **Trp**, **His**, **Tyr**, **Glc**, **Ser**, **DA**, **ASP**, 4 mM for Ca^{2+}, Fe^{3+}, K^{+}, SO_4^{2-}, Na^{+} and Mg^{2+}, respectively.

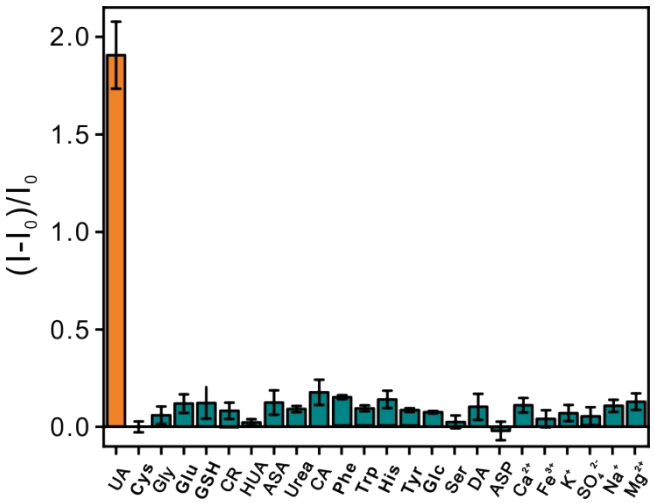

Fig. S42. Fluorescence responses of the **RF@H1** solution upon addition of **UA** or endogenous substances. I_0 and I assigned as the fluorescence intensities of the **RF@H1** reporter pair in the absence and presence of **UA** or endogenous substances. 10 mM PB buffer, pH 7.4, 25 ℃, [**RF**] = 10 μM, [**H1**] = 95 μM, 0.4 mM for **UA**, **Cys**, **Gly**, **Glu**, **GSH**, **CR**, **HUA**, **ASA**, Urea, **CA**, **Phe**, **Trp**, **His**, **Tyr**, **Glc**, **Ser**, **DA**, **ASP**, 4 mM for Ca^{2+}, Fe^{3+}, K^{+}, SO_4^{2-}, Na^{+} and Mg^{2+}, respectively.

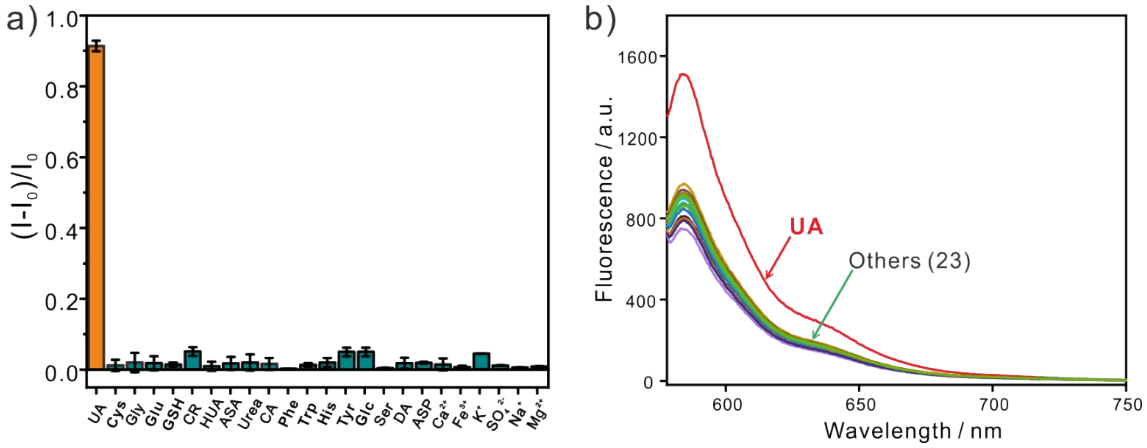

Fig. S43. Fluorescence responses of the **RF@H1** solution upon addition of **UA** or endogenous substances. I_0 and I assigned as the fluorescence intensities of the **RF@H1** reporter pair in the absence and presence of **UA** or endogenous substances. 10 mM PB buffer, pH 7.4, 25 ℃, [**RF**] = 2 μM, [**H1**] = 90 μM, 50 μM for **UA**, **Cys**, **Gly**, **Glu**, **GSH**, **CR**, **HUA**, **ASA**, Urea, **CA**, **Phe**, **Trp**, **His**, **Tyr**, **Glc**, **Ser**, **DA**, **ASP**, 100 μM for Ca^{2+}, Fe^{3+}, K^+, SO_4^{2-}, Na^+ and Mg^{2+}, respectively.

Table S5: Comparison of the developed methods with some other optical methods for determination of uric acid.

Method	Type	Linear range (μM)	LOD (μM)	Reaction time (min)	Ref
Th-MOF-based method	Colormetric	4-70	1.15	18	[3]
Heme-ficin complex-based method		1-120	2.5	210	[4]
Cu^{2+}-TMB–H_2O_2-based method		1-100	6.4	75	[5]
Ag nanoprism-based method		1-40	7.0	40	[6]
Unmodified Ag nanoprism-based method		0.01-3	1.0	15	[7]
Ag@Au NR-based method		0.1-1	6.5	2	[8]
Postfunctionalized MOF-based method	Fluorescence	0.01-400	2.3×10^{-3}	1	[9]
S, N co-doped C-dots-based method		0.08-10/10-50	0.07	45	[10]
DC-biased optofluidic biolaser method		/	3.63	20	[11]
GC5A·Fl complex-based method		0–47.64	1.65	Immediately	[12]
Upconversion NP-based method	colorimetric and fluorometric dual-mode	10-1000	5.79	30	[13]
B,N-carbon dots-based method		100-400/1-500	0.9/1	20	[14]
Tetralactam macrocycle based method		0-90/37-134	1.23/0.33	Immediately	This study

6. Testing of Real Urine Samples

6.1 Detection of Sample by HPLC

UA concentrations in real urine samples were all tested twice by HPLC, the average values and standard deviations are given in Table S3. Errors are smaller than ± 10%.

Table S3. Uric acid concentrations in real urine samples measured by HPLC.

Samples	**UA** (mM)	Samples	**UA** (mM)
1	2.20 ± 0.22	10	3.25 ± 0.17
2	3.35 ± 0.05	11	1.66 ± 0.11
3	6.35 ± 0.01	12	6.79 ± 0.33
4	3.14 ± 0.01	13	0.87 ± 0.00
5	1.37 ± 0.03	14	7.06 ± 0.04
6	4.24 ± 0.18	15	1.40 ± 0.01
7	3.32 ± 0.01	16	1.13 ± 0.03
8	0.88 ± 0.07	17	9.42 ± 0.30
9	7.69 ± 0.28	18	5.20 ± 0.28

6.2 Detection of Sample by Paper Strips

Firstly, **RF@H1** loaded paper strips were prepared. PB buffer (10 mM, pH 7.4) was selected as the solvent to dissolve **RF** and **H1**. 300 μL 50 μM **RF** was dropped on the paper strips, dried at 60 °C. Then 300 μL 100 μM **H1** was dropped on the paper strips which was also dried at 60 °C subsequently. Its linear range and LOD were tested.

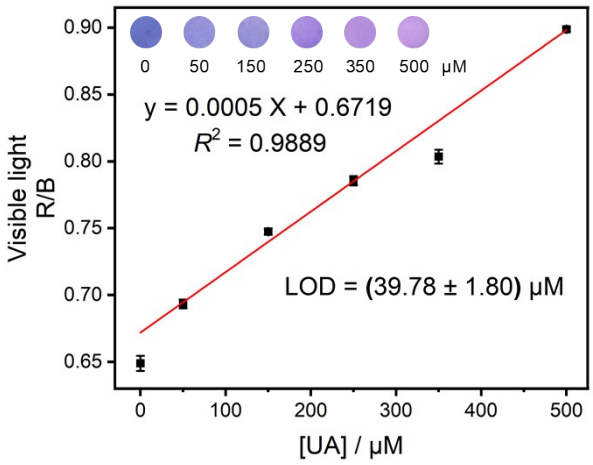

Fig. S44. Digital images of the paper strips in the presence of different concentrations of **UA** under visible light. The linear relationship between R/B value and concentrations of **UA** at 0 - 500 μM.

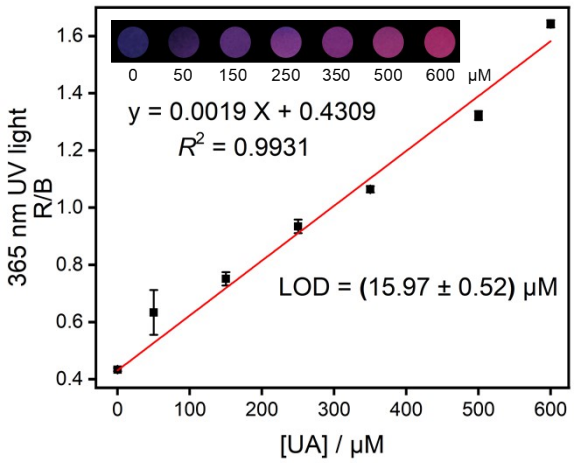

Fig. S45. Digital images of the paper strips in the presence of different concentrations of **UA** under 365 nm UV light. The linear relationship between R/B value and concentrations of **UA** at 0 - 600 μM.

Then we detected the **UA** levels of the real samples by using the prepared paper strips. The pretreated urine sample were diluted 20 times with PB buffer (10 mM, pH 7.4). At last, 18 groups of diluted urine samples were dropped on the paper strips respectively and dried in the oven. The colors of paper strips under visible light and 365 nm UV light were recorded with a camera. The following is the relationship between the normalized R/B value of paper strips and **UA** level determined by HPLC.

Table S4. The relationship between UA level determined by HPLC and the normalized R/B value of paper strips.

		UA (mM)	visible light R/B	365 nm R/B
visible light R/B	Pearson corr. (*r*)	0.9664	--	0.9034
	p-value	< 0.001	--	< 0.001
365 nm R/B	Pearson corr. (*r*)	0.9346	0.9034	--
	p-value	< 0.001	< 0.001	--

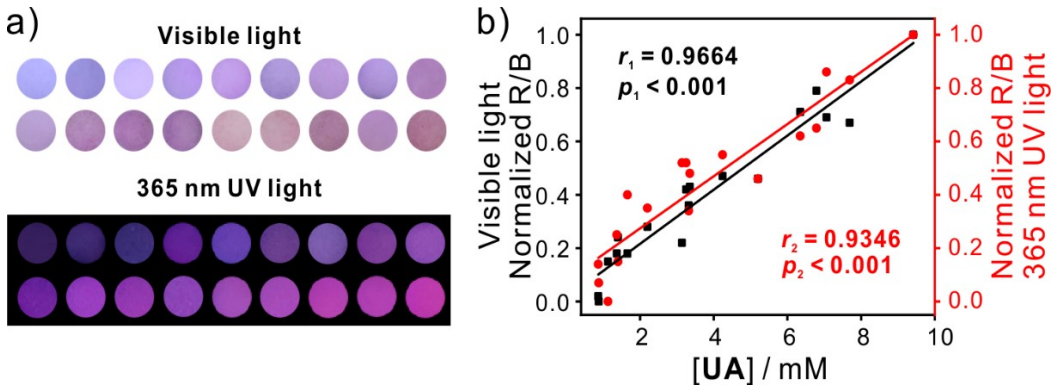

Fig. S46. a) The images of **RF@H1**-loaded paper strips after treatment with the diluted urine from 18 volunteers (arranged from low to high **UA** level) under visible and 365 nm UV light; b) strong positive correlations between **UA** level determined by HPLC and the normalized R/B value of paper strips recorded under visible (r1, p1) and 365 nm UV light (r2, p2).

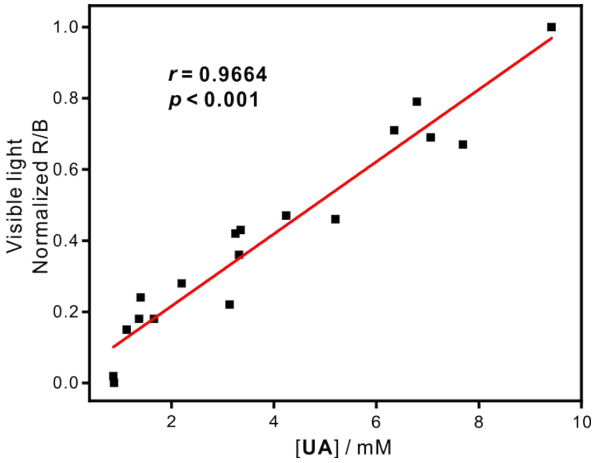

Fig. S47. A high-positive correlation (Pearson correlation coefficient, $r = 0.9664$, $p < 0.001$) of **UA** level determined by HPLC and the normalized value of R/B (the paper strips recorded under visible light).

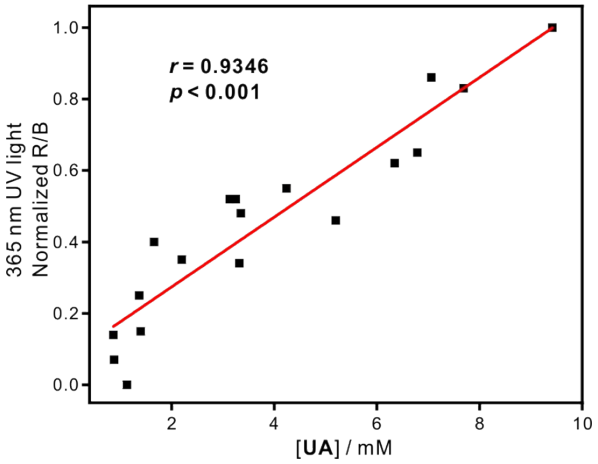

Fig. S48. A high-positive correlation (Pearson correlation coefficient, $r = 0.9346$, $p < 0.001$) of **UA** level determined by HPLC and the normalized value of R/B (the paper strips recorded under 365 nm UV light).

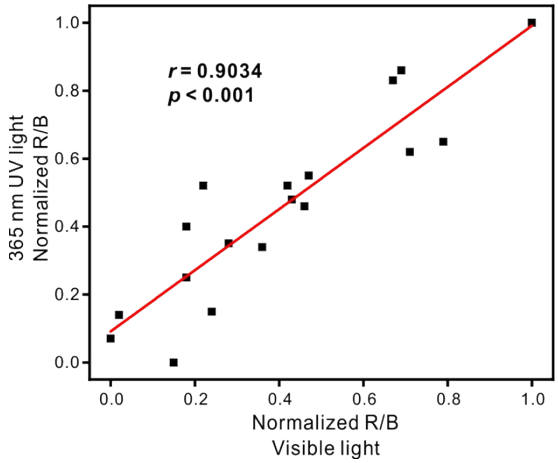

Fig. S49. A high-positive correlation (Pearson correlation coefficient, r = 0.9034, p < 0.001) between the normalized value of R/B value of paper strips recorded under visible light and 365 nm UV light.

7. Computational Data

The calculations were performed using Gaussian 09 package.[15] The geometries of complexes **RF@H1 UA@H1 and PY@H1** have been optimized employing density functional theory (DFT) with dispersion corrected method (ωB97XD)[16] in combination with 6-31G(d,p) basis set. Geometry optimizations were performed by considering the solvent effects (SMD, water) without applying any geometry Constraints. Minima were characterized by the absence of imaginary frequencies. Independent gradient model based on Hirshfeld partition (IGMH) analysis were carried out with Multiwfn 3.7 program.[17] Molecular plots were visualized by the VMD 1.9.3 program.[18]

There is no imaginary frequency after optimization and frequency analysis.

RF@H1

H	4.9031690495	0.2178124923	-1.9914171769
C	4.7922172906	0.2508740077	-0.9150621179
H	4.8637724738	2.3592992743	-0.8932776571
C	4.7624003340	1.4664787508	-0.2870670150
C	4.5749614458	-0.9057970739	1.2104657590
C	4.5836899431	1.5693099489	1.1172373214
C	4.6758868248	-0.9472866072	-0.1694369021
C	4.4920232491	0.3604196759	1.8658440116
C	4.4925349776	2.8348844439	1.7708543821
H	4.2903792729	-0.4200233581	3.8907101052
C	4.2054862267	2.8774078377	3.1232390186
C	4.1435469432	1.6820592438	3.8794680553
H	3.9746009005	1.7167602249	4.9482204299
C	4.3086821147	0.4675683928	3.2705739594
O	4.0015651910	4.1039721873	3.6781934944

O	4.6601241827	-2.1728803255	-0.7637415125
C	3.7888647403	4.2037417775	5.0884117934
H	2.9364574975	3.5817280979	5.3822092568
H	4.6782633757	3.8458815743	5.6202294299
C	4.7701326257	-2.2570223749	-2.1862681478
H	3.9971036624	-1.6408295664	-2.6586757901
H	5.7503308647	-1.8813838321	-2.5027451590
C	4.5918179871	-3.7090699703	-2.5642518550
H	3.6090249085	-4.0711709652	-2.2487511163
H	5.3610716325	-4.3323282464	-2.1003125280
H	4.6680241878	-3.8156702844	-3.6494051220
C	3.5111385302	5.6569707432	5.3966024326
H	2.6159508095	5.9955228868	4.8680772809
H	4.3549356604	6.2880008441	5.1044505679
H	3.3444908080	5.7774933735	6.4700918147
C	4.7436621961	4.1186053139	1.0179911090
H	4.9485063011	4.9196209765	1.7298064763
H	5.6246581537	4.0176954791	0.3831575837
C	4.5582647523	-2.1868101146	2.0080875720
H	4.7899247577	-3.0317270115	1.3587521858
H	5.3252402347	-2.1577647252	2.7863512292
H	-1.9116954433	0.1080527726	-2.9397439559
C	-2.0998552877	0.1398707801	-1.8741328369
H	-2.2412115168	2.2448669107	-1.8819761983
C	-2.2810036479	1.3530381904	-1.2671963512
C	-2.4345938277	-1.0186924694	0.2350466613
C	-2.4957325412	1.4552892770	0.1320958078
C	-2.1536724819	-1.0572830006	-1.1198085472
C	-2.5737389862	0.2466190151	0.8826033986
C	-2.6264761950	2.7202261595	0.7802038795
H	-2.9078980987	-0.5359582982	2.8890292646
C	-2.7209599172	2.7658509919	2.1593850244
C	-2.8300578685	1.5697428638	2.9090516668
H	-2.9604323507	1.6050650758	3.9831714914
C	-2.7842679541	0.3533298466	2.2835500061
O	-2.7151152561	3.9957938128	2.7435295783
O	-1.9375793877	-2.2791424670	-1.6818491260
C	-2.8986799588	4.0960326613	4.1578022809
H	-3.8877005729	3.7079187721	4.4282272985
H	-2.1396264519	3.4999730531	4.6758435841
C	-1.6524095841	-2.3604633800	-3.0800010714
H	-2.5203611990	-2.0145910065	-3.6536585445
H	-0.7996568053	-1.7180858472	-3.3261720270
C	-1.3319131862	-3.8044771606	-3.3885724132

H	-2.1785012870	-4.4537600682	-3.1494865665
H	-0.4616278108	-4.1367326065	-2.8152053702
H	-1.1056204658	-3.9086601919	-4.4528402957
C	-2.7616764075	5.5559412348	4.5237049023
H	-3.5131852426	6.1612774519	4.0095572269
H	-1.7673782632	5.9249253025	4.2581123513
H	-2.8982650020	5.6769479953	5.6013771814
C	-2.7029945019	3.9986699941	-0.0182531139
H	-3.1195528347	4.7896773936	0.6070906042
H	-3.3736102953	3.8727700115	-0.8690021539
C	-2.5957849474	-2.3020327270	1.0125612610
H	-3.5465864538	-2.3006537308	1.5517865748
H	-2.6145960894	-3.1509836943	0.3283714039
H	1.7019781591	6.8710954007	-4.7240773282
C	1.5859457679	6.2805245387	-3.8218926231
C	1.2876365033	4.7711452203	-1.5034868639
C	0.3188760531	5.8818213340	-3.4115931267
C	2.7048459454	5.9202495943	-3.0795719772
C	2.5592694166	5.1681085274	-1.9127936102
C	0.1641327646	5.1295326279	-2.2460903660
H	-0.5578406498	6.1515836892	-3.9898915838
H	3.6971431261	6.2201141533	-3.3977866251
H	1.1770686977	4.1327084878	-0.6350317416
C	-1.2196716813	4.7104061211	-1.8518346982
C	3.7954354214	4.7911790771	-1.1539542972
O	4.8963485575	4.7530702755	-1.7226068179
O	-2.1217880281	4.6400366699	-2.6992200536
N	3.6425560106	4.5206745608	0.1548717864
H	2.7316175658	4.5981855146	0.5815420981
N	-1.4213816254	4.4391151437	-0.5498036584
H	-0.6644175111	4.5434892167	0.1089646889
H	0.1564634321	-2.0627313271	7.4163029806
C	0.3058977477	-2.3102826001	6.3710900068
C	0.6888821944	-2.9480706822	3.6927055906
C	-0.7932229487	-2.4745259874	5.5331627554
C	1.5966161578	-2.4360354098	5.8657223279
C	1.7903448252	-2.7431879675	4.5183688478
C	-0.6020243609	-2.7817192944	4.1854572005
H	-1.8012146628	-2.3472585275	5.9131683644
H	2.4580632200	-2.2786589028	6.5058708723
H	0.8373571106	-3.2423416293	2.6597944049
C	-1.7864690429	-2.8428302334	3.2739784892
C	3.1799210072	-2.7628419107	3.9650796379
O	4.1592193048	-3.0420042557	4.6691077650

O	-2.9114208087	-3.1558834793	3.6851883677
N	3.2778227167	-2.4080400569	2.6677277091
H	2.4609500454	-1.9984260076	2.2305381479
N	-1.5376926409	-2.4855984026	1.9976216236
H	-0.6458705175	-2.0484642372	1.7982065674
O	1.0718039687	2.0820606694	0.3587642946
C	1.1117290754	-0.3072582311	0.3483952752
C	0.8145570355	0.7568527193	2.3607719213
N	0.9232197457	-0.3611583917	1.7092991663
C	0.8860222207	2.0589592404	1.6965025855
C	1.1867460902	0.9176452343	-0.3324627010
C	0.7733302081	3.2258915621	2.3712685465
C	0.5738279657	3.2169307992	3.8059683877
C	0.5014907381	1.9053158777	4.4776048994
C	0.6148197401	0.7530545608	3.7965633776
C	1.3760137972	0.9902270333	-1.7009786631
C	1.4934665349	-0.2036762824	-2.4068345063
C	1.4226837223	-1.4502743848	-1.7538934014
C	1.2339959833	-1.4941256113	-0.3928704930
O	0.4655480837	4.2650068651	4.4627843731
O	1.6779371651	-0.1162353722	-3.7425975213
H	0.8290827488	4.1807170651	1.8601078364
H	0.3518324123	1.9159416995	5.5518495018
H	0.5621496793	-0.2123175752	4.2867934472
H	1.4306786544	1.9480711576	-2.2046724401
H	1.5177481321	-2.3646640899	-2.3312132933
H	1.1760352115	-2.4416104477	0.1333093926
H	1.7450265087	-1.0021441647	-4.1221794256

PY@H1

H	0.955943921	-3.499679231	3.708147052
C	0.776480974	-2.432204439	3.702379621
H	2.836206549	-2.007678106	3.50418552
C	1.842063443	-1.581638512	3.587373093
C	-0.766156354	-0.56227168	3.834798993
C	1.660887501	-0.17475473	3.527855698
C	-0.543506001	-1.928186232	3.804393521
C	0.332768605	0.329101887	3.646835553
C	2.756739557	0.718836823	3.334227057
H	-0.849414051	2.154028497	3.66189705
C	2.505917166	2.069466282	3.173855949
C	1.191145173	2.578502759	3.309788694
H	1.000500461	3.639815725	3.213358507

C	0.143774088	1.733190779	3.557488315
C	-2.148205383	-0.036260306	4.134036078
H	-2.103000155	0.715849611	4.926205053
H	-2.775323164	-0.853926839	4.494870421
C	4.186297014	0.222903048	3.302350354
H	4.855352882	1.043187766	3.564466566
H	4.336548613	-0.574892503	4.030085208
N	-2.780134277	0.59995726	2.987558857
H	-2.542319415	0.255325806	2.071534691
N	4.59058062	-0.309560704	2.005692934
H	4.824202711	0.362383587	1.291469332
C	-3.563955034	1.696075668	3.110608349
C	4.930345572	-1.608515755	1.817174714
O	-3.763366009	2.255106519	4.187771642
O	4.933626645	-2.438004847	2.725666385
C	-4.159577773	2.21780622	1.834772494
C	-5.203340968	3.274896082	-0.531516607
C	-4.558173419	3.553770932	1.777320345
C	-4.319177265	1.410200663	0.711947185
C	-4.804334314	1.939362041	-0.482417271
C	-5.087907728	4.075694445	0.601060776
H	-4.445362231	4.172180571	2.660767233
H	-4.097091086	0.350572898	0.769582993
H	-5.394491796	5.115173938	0.5612421
H	-5.594370812	3.675626024	-1.460319889
H	-0.891580796	3.323144883	-3.692675691
C	-0.602892477	2.281245064	-3.638038782
H	-2.604599097	1.654549839	-3.400274334
C	-1.57313464	1.330589111	-3.471463916
C	1.114023451	0.565742146	-3.757039286
C	-1.250849507	-0.045816946	-3.371269251
C	0.756614934	1.905237545	-3.753322065
C	0.114659691	-0.423720694	-3.519009938
C	-2.255115185	-1.040304118	-3.138256618
H	1.47251878	-2.127349408	-3.504835327
C	-1.874698385	-2.355233445	-2.997444785
C	-0.518840473	-2.738444779	-3.136949883
H	-0.249442435	-3.780278823	-3.000587686
C	0.441616296	-1.80654766	-3.409590568
C	2.528985973	0.175218579	-4.104128889
H	3.070642759	1.04970283	-4.46642318
H	2.518980963	-0.5566966	-4.920592303
C	-3.705287386	-0.650917996	-3.007909394
N	3.25151878	-0.409173433	-2.980006442

H	2.752898193	-0.525160331	-2.112343707
N	-3.910990499	0.146255905	-1.804236798
H	-3.129284526	0.211880255	-1.168181992
C	4.399325196	-1.0998221	-3.189671796
C	-4.866516669	1.106665818	-1.729222801
O	4.921846602	-1.178692545	-4.298397613
O	-5.691550411	1.302965515	-2.616164159
C	4.976966973	-1.790404745	-1.989828035
C	5.939507429	-3.212976775	0.205785531
C	5.706869237	-2.963236485	-2.180769394
C	4.777327359	-1.309592105	-0.698341547
C	5.241813361	-2.020892752	0.40683285
C	6.189378296	-3.669253589	-1.083576776
H	5.874470198	-3.319655671	-3.191087413
H	4.256386187	-0.367894753	-0.568254133
H	6.746557078	-4.587390727	-1.23367085
H	6.27908367	-3.772248046	1.070143823
H	-4.322111444	-1.550565453	-2.9726219
H	-4.032083174	-0.057710679	-3.868620317
O	-2.805059256	-3.296690882	-2.647498294
C	-3.046300999	-4.32386821	-3.614470261
H	-2.110811792	-4.843809919	-3.852687978
O	3.571148288	2.857545768	2.872250888
O	-1.630805011	-2.737300373	3.887965543
C	3.392607077	4.268024614	2.78278807
H	2.635940473	4.499320403	2.023651655
H	3.043458508	4.661049216	3.745643463
C	-1.445563171	-4.148043187	3.941238623
H	-0.897210773	-4.483251637	3.052068501
H	-0.854103376	-4.414535467	4.825788278
O	1.753098917	2.812114228	-3.893339549
C	1.436576256	4.200434455	-3.867730015
H	0.842279512	4.463994146	-4.751155499
H	0.837804249	4.426042609	-2.977206831
C	2.742931974	4.96303244	-3.840448602
H	3.342997568	4.735567957	-4.724826156
H	3.320066682	4.702464866	-2.949275995
H	2.542585333	6.037313065	-3.824448537
H	-3.422942148	-3.863948131	-4.536798253
C	-4.058071953	-5.283253748	-3.028756913
H	-4.278600224	-6.075601203	-3.748178216
H	-4.989157523	-4.763499404	-2.787969219
H	-3.668457898	-5.743381423	-2.116948144
C	-2.816970479	-4.784570369	3.993397312

H	-3.362145717	-4.459511288	4.882718921
H	-2.71825902	-5.872508745	4.023588883
H	-3.397994213	-4.514043548	3.108363298
C	4.727714429	4.868047721	2.399599618
H	5.060778178	4.475859411	1.435239609
H	5.485625254	4.638283622	3.152558314
H	4.634782639	5.953805322	2.319365463
C	-0.452588283	1.225822051	-0.015154694
C	0.932643535	0.942856564	0.087822613
O	-1.361203322	0.217144855	0.093301259
C	-0.947785455	2.491178554	-0.208162184
C	1.331049424	-0.37683097	0.294052159
C	1.820289535	2.045118519	-0.03042346
C	-0.975116185	-1.080416592	0.231969257
C	-0.046123271	3.571750108	-0.347988687
C	0.400737404	-1.407597875	0.321039057
C	1.360148216	3.30784205	-0.248786911
C	-1.973571006	-2.018503394	0.289153111
N	-0.491645002	4.822494153	-0.582466732
C	0.725425361	-2.786641489	0.43828455
C	-1.63430591	-3.387783427	0.4004912
C	0.41964456	5.960379793	-0.528169824
C	-1.919219674	5.069693325	-0.728344569
C	-0.242763818	-3.743106903	0.458942229
N	-2.591775998	-4.329150647	0.451617769
H	-2.018802608	2.627827251	-0.261634017
H	2.382202198	-0.608386969	0.436488391
H	2.88791983	1.875301627	0.049278053
H	2.071964672	4.115246339	-0.354601511
H	-3.00197021	-1.701703947	0.191503518
H	1.770747069	-3.068098725	0.506564622
H	-0.154952197	6.876699177	-0.643450763
H	0.94204179	6.002773146	0.432506475
H	1.161209288	5.924559762	-1.332515071
H	-2.073383975	6.097926374	-1.048484487
H	-2.349281846	4.410738651	-1.488441324
H	-2.452187703	4.911299658	0.215301654
H	0.046631503	-4.782489076	0.531761567
C	-2.245365521	-5.744859686	0.479593177
H	-3.161275617	-6.331165181	0.507560366
H	-1.661076874	-5.994491796	1.370453507
H	-1.677359962	-6.03214057	-0.411035971
C	-3.99407858	-3.941926426	0.353778322
H	-4.190434271	-3.457621876	-0.607940581

H	-4.266957537	-3.262915534	1.168121396
H	-4.61543491	-4.831555964	0.431365355

UA@H1

H	3.213456101	0.68653809	3.440069216
C	2.200944402	0.303647018	3.47577383
H	1.383501677	2.244059452	3.624293169
C	1.159079476	1.185682833	3.566095466
C	0.675715916	-1.5875941	3.527543958
C	-0.189003667	0.736989498	3.603482695
C	1.963142861	-1.092459492	3.425724289
C	-0.418339784	-0.670181368	3.606969394
C	-1.284434118	1.65187319	3.655249319
H	-1.981852969	-2.175583147	3.785842624
C	-2.577784881	1.159858536	3.695967848
C	-2.808076133	-0.23638084	3.747052557
H	-3.816663443	-0.623271367	3.821034473
C	-1.76137375	-1.117677064	3.712596036
C	0.444067061	-3.083318376	3.57841967
H	-0.146935314	-3.352412073	4.456860715
H	1.405628949	-3.592774096	3.654885481
C	-1.055343774	3.144897717	3.689412772
H	-2.004801273	3.654772934	3.85679848
H	-0.387820308	3.416506061	4.511550121
N	-0.285549853	-3.57767948	2.420707569
H	0.059922735	-3.29178801	1.513196262
N	-0.433501486	3.638922917	2.467663097
H	-0.692350952	3.182057886	1.597822622
C	-1.451196453	-4.254582048	2.523921603
C	0.651559643	4.443983575	2.507674796
O	-1.94669401	-4.57295079	3.607534248
O	1.132377425	4.87912904	3.554647688
C	-2.174727769	-4.515203918	1.233271006
C	-3.642126284	-4.741939501	-1.128288345
C	-3.544422749	-4.777512301	1.281511006
C	-1.541727919	-4.414369555	-0.001986172
C	-2.272671712	-4.480930095	-1.18486178
C	-4.270596748	-4.907687612	0.1019561
H	-4.027603563	-4.861252984	2.248598223
H	-0.468149834	-4.290992715	-0.040569506
H	-5.335297387	-5.111027144	0.142138938
H	-4.201811411	-4.797912008	-2.055296731
H	-3.975697971	-0.446621018	-3.938515621

C	-2.955159686	-0.095523273	-3.851217144
H	-2.195405873	-2.064662681	-3.864111713
C	-1.940540961	-1.012909989	-3.800724888
C	-1.370128209	1.740328754	-3.717257391
C	-0.585199829	-0.610355345	-3.672294737
C	-2.677525307	1.292380011	-3.798291088
C	-0.308710464	0.78782458	-3.636413946
C	0.475142579	-1.564141152	-3.587752613
H	1.31293498	2.237833436	-3.543453192
C	1.77209285	-1.118359461	-3.41035535
C	2.057584786	0.26916229	-3.398346701
H	3.077480454	0.618545524	-3.29498996
C	1.050359609	1.187466435	-3.523519045
C	-1.088178534	3.224179579	-3.748298096
H	-2.015082884	3.767309312	-3.936351636
H	-0.397363221	3.467440572	-4.56086615
C	0.197947811	-3.04853141	-3.686971051
N	-0.469688779	3.700167799	-2.517220335
H	-0.69442374	3.200517898	-1.661338517
N	-0.45886304	-3.561719724	-2.49520184
H	-0.018987884	-3.324523565	-1.613664422
C	0.60999308	4.513263873	-2.551242664
C	-1.655704375	-4.186434434	-2.523633961
O	1.067029795	4.985617088	-3.592530438
O	-2.255718435	-4.441671498	-3.571020114
C	1.292109374	4.732734833	-1.232714381
C	2.696531769	4.883661214	1.171388986
C	2.675359995	4.918671219	-1.237648988
C	0.608413122	4.665002501	-0.020104046
C	1.311560297	4.700649059	1.184155084
C	3.374469834	5.002485978	-0.03788025
H	3.191260941	4.975972748	-2.189528305
H	-0.471102353	4.569508383	-0.013533077
H	4.450426361	5.136465183	-0.045040934
H	3.22793442	4.91312835	2.115931891
H	1.137484663	-3.580019186	-3.846154247
H	-0.457448143	-3.268611313	-4.531719073
O	2.739046096	-2.061221248	-3.240752872
C	4.107545897	-1.675597224	-3.317471014
H	4.357714595	-0.996765716	-2.492743299
O	-3.58819694	2.067031036	3.707049166
O	2.975938738	-1.988176795	3.259855466
C	-4.93789425	1.61308641	3.730513736
H	-5.129207863	0.966055039	2.865427068

H	-5.121157733	1.03081344	4.642105677
C	4.305136542	-1.600767189	3.606810863
H	4.662498726	-0.81126016	2.93566285
H	4.317010849	-1.210954274	4.631844286
O	-3.656077906	2.233579267	-3.839718569
C	-5.018644578	1.825750216	-3.909539501
H	-5.189063189	1.243779427	-4.82386124
H	-5.263437957	1.191751366	-3.048259419
C	-5.864508493	3.081243261	-3.907988561
H	-5.622268749	3.710155972	-4.768288116
H	-5.696816372	3.657039537	-2.994408453
H	-6.92263405	2.81349895	-3.960699308
H	4.292443473	-1.144199894	-4.258929154
C	4.940463238	-2.935893514	-3.23342196
H	6.001792614	-2.680023041	-3.275757622
H	4.709374717	-3.606946702	-4.064151589
H	4.749915334	-3.464474543	-2.296223485
C	5.183414024	-2.824694485	3.469296909
H	4.829037896	-3.631880628	4.114892706
H	6.208736495	-2.574618621	3.752500539
H	5.191261332	-3.175152033	2.434222147
C	-5.82517027	2.838977227	3.690182613
H	-5.644991249	3.414683485	2.778931828
H	-5.634688363	3.48085106	4.553911278
H	-6.87483862	2.535696757	3.707793995
C	4.195333581	-0.939421938	0.242582938
N	3.580588064	0.303489554	0.248426422
C	1.938753048	-1.989179112	-0.041540999
C	2.23388077	0.406798782	0.110936251
N	3.325217713	-2.004142785	0.082595272
C	1.414150457	-0.673509656	-0.03778652
O	5.396312145	-1.079101217	0.368466522
H	3.755667475	-2.91940151	0.116301187
O	1.30857479	-3.046620534	-0.129518115
H	4.176734947	1.112536021	0.354533834
N	0.113961531	-0.181922182	-0.121289987
H	-0.725337467	-0.722993598	-0.256340246
N	1.469047956	1.527127006	0.10830691
H	1.778638804	2.480122728	0.243196924
C	0.123645701	1.174216761	-0.029951469
O	-0.830560237	1.952610063	-0.054538677

8. References

[1] H. Zhang, L.-L. Wang, X.-Y. Pang, L.-P. Yang, W. Jiang, *Chem. Commun.*, 2021, **57**, 13724–13727.

[2] a) H. Bakirci and W. M. Nau, *Adv. Funct. Mat.* 2006, **16**, 237-242. b) A. Hennig, H. Bakirci, W. M. Nau, *Nat. Methods.*, 2007, **4**, 629-632

[3] A. Badoei-dalfard, N. Sohrabi, Z. Karami and G. Sargazi, *Biosens. Bioelectron.*, 2019, **141**, 111420.

[4] Y. Pan, Y. Yang, Y. Pang, Y. Shi, Y. Long and H. Zheng, *Talanta*, 2018, **185,** 433-438.

[5] H.-F. Lu, J.-Y. Li, M.-M. Zhang, D. Wu and Q.-L. Zhang, *Sens. Actuators B Chem.*, 2017, **244**, 77-83.

[6] D. Wu, H.-F. Lu, H. Xie, J. Wu, C.-M. Wang and Q.-L. Zhang, *Sens. Actuators B Chem.*, 2015, **221**, 1433-1440.

[7] K. Tan, G. Yang, H. Chen, P. Shen, Y. Huang and Y. Xia, *Biosens. Bioelectron.*, 2014, **59**, 227-232.

[8] M. Amjadia, T. Hallaja and E. Nasirloo, *Microchem. J*., 2020, **154**, 104642.

[9] S.-M. Qu, Z. Li and Q. Jia, *ACS Appl. Mater. Interfaces.*, 2019, **11**, 34196−34202.

[10] H.-Y. Wang, Q.-J. Lu, Y.-X. Hou, Y.-L. Liu and Y.-Y. Zhang, *Talanta*, 2016, **155**, 62-69.

[11] Y.-Q. Wang, X. Yang, C.-Y. Gong, J.-G. Mao, Y. Wu, G.-L. Yin, T. Zhu, G.-D. Peng, Y.-J. Rao and Y. Gong, *J. Lightw. Technol.*, 2020, **38**, 1557-1563.

[12] Y. Zhang, H. Yu, S. Chai, X. Chai, L. Wang, W.-C. Geng, J.-J. Li, Y.-X. Yue, D.-S. Guo and Y. Wang, *Adv. Sci*., 2022, **9**, e2104463.

[13] A. Fang, Q. Wu, Q. Lu, H. Chen, H. Li, M. Liu, Y. Zhang and S. Yao, *J. Mol. Graph. Model.*, 1996, **14**, 33−38.

[14] N. Xiao, S.-G. Liu, S. Mo, Y.-Z. Yang, L. Han, Y.-J. Ju, N.-B. Li and H.-Q. Luo, *Sens. Actuators B Chem.*, 2018, **273**, 1735-1743.

[15] *Gaussian 09, Revision D.01*, M. J. Frisch, G. W. Trucks, H. B. Schlegel, G. E. Scuseria, M. A. Robb, J. R. Cheeseman, G. Scalmani, V. Barone, B. Mennucci, G. A. Petersson, H. Nakatsuji, M. Caricato, X. Li, H. P. Hratchian, A. F. Izmaylov, J. Bloino, G. Zheng, J. L. Sonnenberg, M. Hada, M. Ehara, K. Toyota, R. Fukuda, J. Hasegawa, M. Ishida, T. Nakajima, Y. Honda, O. Kitao, H. Nakai, T. Vreven, J. A. 10 Montgomery, J. E. Peralta, F. Ogliaro, M. Bearpark, J. J. Heyd, E. Brothers, K. N. Kudin, V. N. Staroverov, R. Kobayashi, J. Normand, K. Raghavachari, A. Rendell, J. C. Burant, S. S. Iyengar, J. Tomasi, M. Cossi, N. Rega, J. M. Millam, M. Klene, J. E. Knox, J. B. Cross, V. Bakken, C. Adamo, J. Jaramillo, R. Gomperts, R. E. Stratmann, O. Yazyev, A. J. Austin, R. Cammi, C. Pomelli, J. W. Ochterski, R. L. Martin, K. Morokuma, V. G. Zakrzewski, G. A. Voth, P. Salvador, J. J. Dannenberg, S. Dapprich, A. D. Daniels, O. Farkas, J. B. Foresman, J. V. Ortiz, J. Cioslowski, D. J. Fox, Gaussian, Inc.: Wallingford CT, USA, 2013.

[16] a) J.-D. Chai and M. Head-Gordon, *Phys. Chem. Chem. Phys.*, 2008, **10**, 6615–6620; b) A. V. Marenich, C. J. Cramer and D. G. Truhlar, *J. Phys. Chem. B*, 2009, **113**, 6378–6396; c) J. C. Kromann, C. Steinmann and J. H. Jensen, *J. Chem. Phys.*, 2018, **149**, 104102.

[17] a) T. Lu and Q. Chen, *J. Comput. Chem.*, 2022, **43**, 539–555; b) T. Lu and F. Chen, *J. Comput. Chem.*, 2012, **33**, 580–592.
[18] W. Humphrey, A. Dalke, K. Schulten, *J. Mol. Graph. Model.*, 1996, **14**, 33−38.